This is the Pre-Published Version.

This document is the Accepted Manuscript version of a Published Work that appeared in final form in Inorganic Chemistry, copyright © American Chemical Society after peer review and technical editing by the publisher. To access the final edited and published work see https://doi.org/10.1021/acs.inorgchem.8b01684.

TITLE PAGE

Dicopper(I) Complexes Incorporating Acetylide-functionalized Pyridinyl-based Ligands: Synthesis, Structural and Photovoltaic Studies

Maharaja Jayapal,[†] Ashanul Haque,[†] Idris J. Al-Busaidi,[†] Nawal Al-Rasbi,[†] Mohammed K. Al-Suti,[†] Muhammad S. Khan,*[,†] Rayya Al-Balushi,[‡] Shahidul M. Islam,*[, §]Chenghao Xin,[⊥] Wenjun Wu,*[, ⊥] Wai-Yeung Wong,*[,#] Frank Marken*[,└] and Paul R. Raithby*[,└]

[†] Department of Chemistry, Sultan Qaboos University, P.O. Box 36, Al Khod 123, Sultanate of Oman. *E-mail:msk@squ.edu.om

[‡] Department of Basic Sciences, College of Applied and Health Sciences, Al-Sharqiyah University, Ibra, Sultanate of Oman.

[§]Department of Chemistry, University of Illinois at Chicago, Chicago, IL 60607, USA. *E-mail: mshahidi@uic.edu

[⊥]Key Laboratory for Advanced Materials and Institute of Fine Chemicals, Centre for Computational Chemistry, Shanghai Key Laboratory of Functional Materials Chemistry, School of Chemistry and Molecular Engineering, East China University of Science and Technology, Shanghai 200237, China. *E-mail: wjwuecust@gmail.com

[#]Institute of Molecular Functional Materials and Department of Applied Biology and Chemical Technology, The Hong Kong PolytechnicUniversity, Hung Hom, Kowloon, Hong Kong. *E-mail:wai-yeung.wong@polyu.edu.hk

[└]Department of Chemistry, University of Bath, Claverton Down, Bath BA2 7AY, UK. *E-mail:f.marken@bath.ac.uk,p.r.raithby@bath.ac.uk

Keywords: Acetylide, copper(I), self-assembly, dye-sensitized solar cell and power conversion efficiency.

Dicopper(I) Complexes Incorporating Acetylide-functionalized Pyridinyl Ligands: Synthesis, Structural and Photovoltaic Studies[†]

Maharaja Jayapal,[†] Ashanul Haque,[†] Idris J. Al-Busaidi,[†] Nawal Al-Rasbi,[†] Mohammed K. Al-Suti,[†] Muhammad S. Khan,*[,†] Rayya Al-Balushi,[‡] Shahidul M. Islam,*[, §] Chenghao Xin,[⊥] Wenjun Wu,*[, ⊥] Wai-Yeung Wong,*[,#] Frank Marken*[,∟] and Paul R. Raithby*[,∟]

ABSTRACT

Hetero-aryl incorporated acetylide-functionalized pyridinyl ligands (**L1-6**) with the general formula Py-C≡C-Ar (Py = pyridine and Ar = *thiophene-2-yl*, *2,2'-bithiophene]-5-yl*, *2,2':5',2''-terthiophene]-5-yl*, *thieno[2,3-b]thiophen-2-yl*, *quinoline-5-yl,benzo[c][1,2,5]thiadiazole-5-yl*) have been synthesized by Pd(0)/Cu(I)-catalyzed cross-coupling reaction of 4-ethynylpyridine and the respective heteroaryl halide. **L1-L6** were isolated in respectable yields and characterized by microanalysis, IR spectroscopy, ^{1}H NMR spectroscopy and ESI-MS mass spectrometry. A series of dinuclear Cu(I) complexes **1**-**10** have been synthesized by reacting **L1-L6** with CuI and triphenylphosphine (PPh_3) (**R1**) or with an anchored phosphine derivative, 4-(diphenyl phosphino) benzoic acid (**R2**)/2-(diphenylphosphino)benzenesulfonic acid (**R3**), in a stoichiometric ratio. The complexes are soluble in common organic solvents and have been characterized by analytical, spectroscopic and computational methods. Single crystal X-ray structure analysis confirmed rhomboid dimeric structures for complexes **1**, **2**, **4**, and **5**, and a polymeric structure for **6**. Complexes **1**-**6** showed oxidation potential responses close to 0.9 V *vs*. $Fc^{0/+}$, which were chemically irreversible and are likely to be associated with multiple steps and core oxidation. Preliminary photovoltaic (PV) results of these new materials indicated moderate power conversion efficiency (PCE) in the range of 0.15-1.56% in dye-sensitized solar cells (DSSCs). The highest PCE was achieved with complex **10** bearing the sulfonic acid anchoring functionality.

[†] CCDC reference numbers 1834959-1834963. For crystallographic data in CIF or other electronic formats see DOI: xxxxxx.

INTRODUCTION

Transition metal complexes have attracted significant attention due to their intriguing architectures, topologies and opto-electronic (OE) properties.[1-3] In these complexes, the redox-active metal centers are responsible for different shapes, sizes and geometries, while the organic part tunes and controls photo-physical and physico-chemical properties.[4-5] Furthermore, interaction between metal and conjugated organic spacers imparts low-energy electronic transition to the molecules.[6] Among different transition metals, the monovalent copper (Cu(I)) ion has emerged as a potential candidate for the development of a new generation hybrid materials. High abundance, a diverse set of emission origins (metal-to-ligand charge transfer MLCT, halide-to-ligand charge transfer XLCT, ligand-to-ligand charge transfer LLCT, and ligand-centered (LC) and cluster-centered (CC) states), the ability to harvest singlet and triplet excitons *via* thermally-activated delayed fluorescence (TADF), enlarged exciton diffusion length with reduced charge recombination, and the ability to form mono- to polynuclear complexes are some of the intriguing features offered by Cu(I) based complexes.[7-9] These features prompted researchers to synthesize new Cu(I) complexes for organic light-emitting diodes (OLEDs), light to electricity conversion, light-emitting electrochemical cells, etc. applications.[3, 9] Among carbon (C), nitrogen (N), oxygen (O), phosphorus (P) based donor ligands/co-ligands, N-donating bridging and terminal ligands are most commonly employed to satisfy coordination sphere around Cu(I). This is, essentially, attributed to the versatility, easy complexation (solid as well as solution phase) and exceptional stability offered by N-donors.[10] It has been demonstrated that by fine tuning of the coordinated ligands, a range of complexes could be achieved with unique and controlled photo-physical properties and applications.[3, 11] Furthermore, using designer ligands, the photonic harvesting can be improved and redox potential can be modulated. Following the seminal work by Savage *et al*.[12], significant research efforts have been dedicated to explore the potential of Cu(I) complexes as sensitizer for DSSC.[13-16] Cu(I) complexes are considered potential alternative to the traditional expensive Ru(II) complexes owing to the similarity in photophysical properties of Cu(I) complexes to the latter. Such Cu complexes can also be used in an electrolyte based on the redox potential and frontier orbital (HOMO and LUMO) energy levels of the complexes with respect to the dye materials.[17-18] However, the PCE of most Cu(I) complexes are still below the threshold for commercial application and therefore, the design and development of new Cu(I) complexes for

DSSC application are receiving intense interests from researchers worldwide. Recently, we reported the unique structure and electrochemical properties of Cu(I) dimers and tetramers with ferrocene (Fc) appended ethynylpyridinyl ligands.[19-20] Despite the fact that these dimers and tetramers are easy to synthesize, stable, and possess intriguing OE properties, the presence of the Fc moiety was considered disadvantageous in terms of photo-physical properties for light harvesting applications as Fc is a known luminescence qunecher.[21-23] Based on this notion, we and others reported the PL properties and applications of several mono, di- and polynuclear pyridine-based Cu(I) complexes and decided to replace the Fc moiety by conjugated spacers in the acetylide-functionalized pyridinyl-ligands.[3, 9]

Herein we report the synthesis, structural and photo-physical characterization of a series of new dinuclear Cu(I) complexes **1**-**6** incorporating non-fused/fused heteroarylethynylpyridinyl-based conjugated ligands. Among the heterocyclic spacers, benzothiadiazole and thiophene-based materials have been widely studied for making low band-gap (E_g) complexes/polymers as a result of strong donor (D) and acceptor (A) interactions in the hybrid spacer.[16] Also, these spacers are known to lower the polarity and enhance the solubility of the polymer materials.[17] In order to be used in DSSCs the complexes require anchoring groups in order to bind to the TiO_2 and facilitate electron injection. For this purpose, Cu(I) complexes (**7**-**10**) of heteroarylethynylpyridinyl ligands (**L1**-**L3** and **L6**) incorporating sulfonic acid/carboxylic acid anchored triphenylphosphine auxiliaries have also been synthesized. DSSC devices have been fabricated with these anchored Cu(I) complexes and their performance has been evaluated.

RESULTS AND DISCUSSION

Synthesis and spectroscopic characterization

The synthesis of heteroarylethynylpyridinyl ligands (**L1**-**L6**) and the corresponding Cu(I) complexes was achieved by adaptation of previously reported methods.[24] Briefly, the key protected ligand precursor 4-(trimethylsilylethynyl)pyridine (**P1**) was obtained by the Pd(0)/Cu^I-catalyzed cross-coupling reaction of 4-iodopyridine with trimethylsilylacetylene (TMSA) in $^iPr_2NH$/THF (**Scheme 1**). The ligand precursor, **P1**, was deprotected by aqueous KOH in MeOH/THF followed by purification by silica gel column chromatography yielding 4-ethynylpyridine(**P2**) as an off-white powder in a respectable yield (85-86%). It should be noted that both the trimethylsilyl-protected (**P1**) and the terminal ethynylpyridinyl (**P2**) ligand precursors are somewhat unstable,

decomposing at room temperature and, therefore, were used quickly for the next sequence of reactions. A Sonogashira cross-coupling reaction between **P2** and a heteroaryl halide (**Ar-X**) produced heteroarylethynylpyridinyl ligands (**L1**-**L6**) as light to dark yellow solids in good to moderate yields (75-88%). The Cu(I) complexes (**1-10**) were synthesized by reacting equimolar quantity of the ligands (**L1-L6**), co-ligand (PPh_3/$PPh_2(C_6H_4COOH)$/ $PPh_2(C_6H_4SO_3H)$ and CuI in dry CH_2Cl_2, under argon atmosphere for 24 h. All the complexes are stable to light and air at ambient temperature.

All the synthesized materials were characterized by IR, NMR (^1H, ^{13}C, and ^{31}P) spectroscopy, electron-impact/electrospray ionization mass spectrometry (EI-MS/ESI-MS), and elemental analysis. A sharp peak at around 2165 cm^{-1} in the IR spectrum indicated the formation of 4-(trimethylsilylethynyl)pyridine in the initial cross-coupling reaction. Base-induced deprotection in the second reaction step was confirmed by the expected lowering of the -C≡C- stretching frequency (2096 cm^{-1}) as well as the presence of a new peak at 3223 cm^{-1}, corresponding to free ethynyl proton stretching (-C≡**C-H** str.). The observed $\nu_{(C\equiv C)}$ stretching frequencies of the acetylide-functionalized arylpyridine ligands **L1**-**L6** are 2203, 2197, 2194, 2198, 2217 and 2215cm^{-1}, respectively. This trend clearly shows the impact of employing fused and non-fused thiophene spacers on the values of $\nu_{(C\equiv C)}$ stretching frequencies. For example, a decrease in the values of $\nu_{(C\equiv C)}$ stretching frequency on going from **L1**→**L3** can be attributed to increased conjugation, and hence the donacity (i.e. the order of donacity: **L3** > **L2** > **L1**). It is notable that **L4** bearing fused thiophene (thieno[2,3-*b*]thiophene) has $\nu_{(C\equiv C)}$ stretching frequency value close to its structural analogue **L2** (non-fused system). Comparatively higher values of $\nu_{(C\equiv C)}$ frequency in the case of **L5** and **L6** can be ascribed to electron-withdrawing ('acceptor') ability of quinoline and benzo[c][1,2,5]thiadiazole units. Upon complexation, the single sharp peak in the IR spectrum due to $\nu_{(C\equiv C)}$ in the ligand (**L**) showed only a minor change, possibly due to the large distance between -C≡C- and Cu(I) coordination center.[19] All anchored complexes displayed a $\nu_{(C\equiv C)}$ stretching frequency in the range of 2193-2214 cm^{-1}. Complexes **C7**-**C10** showed a sharp peak in the range of 1701-1723 cm^{-1}, owing to the -C=O functionality. In addition, a broad peak in the range of 3057-3061 cm^{-1}corresponding to -OH carboxylic or sulfonic acid moiety (in case of **R2** or **R3**) was also observed. Similarly, sharp peaks were observed in the range of 1158-1482 cm^{-1} corresponding to S=O groups of **R3** in complexes **C9** and **C10**.

The ^{1}H NMR spectrum of **P1** showed doublets at δ7.22, and δ7.28 ppm corresponding to the α and β protons of the pyridinyl unit, respectively. As expected, for trimethylsilyl (TMS) groups, the singlet appeared at δ0.27 ppm. Both α and β protons of pyridinyl unit in the non-fused/fused heteroarylethynylpyridinyl-based ligands (**L1-L6**) showed only a small shift in their ^{1}H NMR spectra compared to their precursors. Signals due to triphenylphosphine (PPh_3-H) were observed in the δ7-9 ppm region as multiplets.[25-26] The complexes were further characterized by ^{31}P-NMR. All complexes exhibited ^{31}P-NMR peaks between *δ* 29.09-29.24 ppm, which is well documented for ethynylpyridinyl based Cu(I) complexes bearing phosphine auxiliaries.[19]

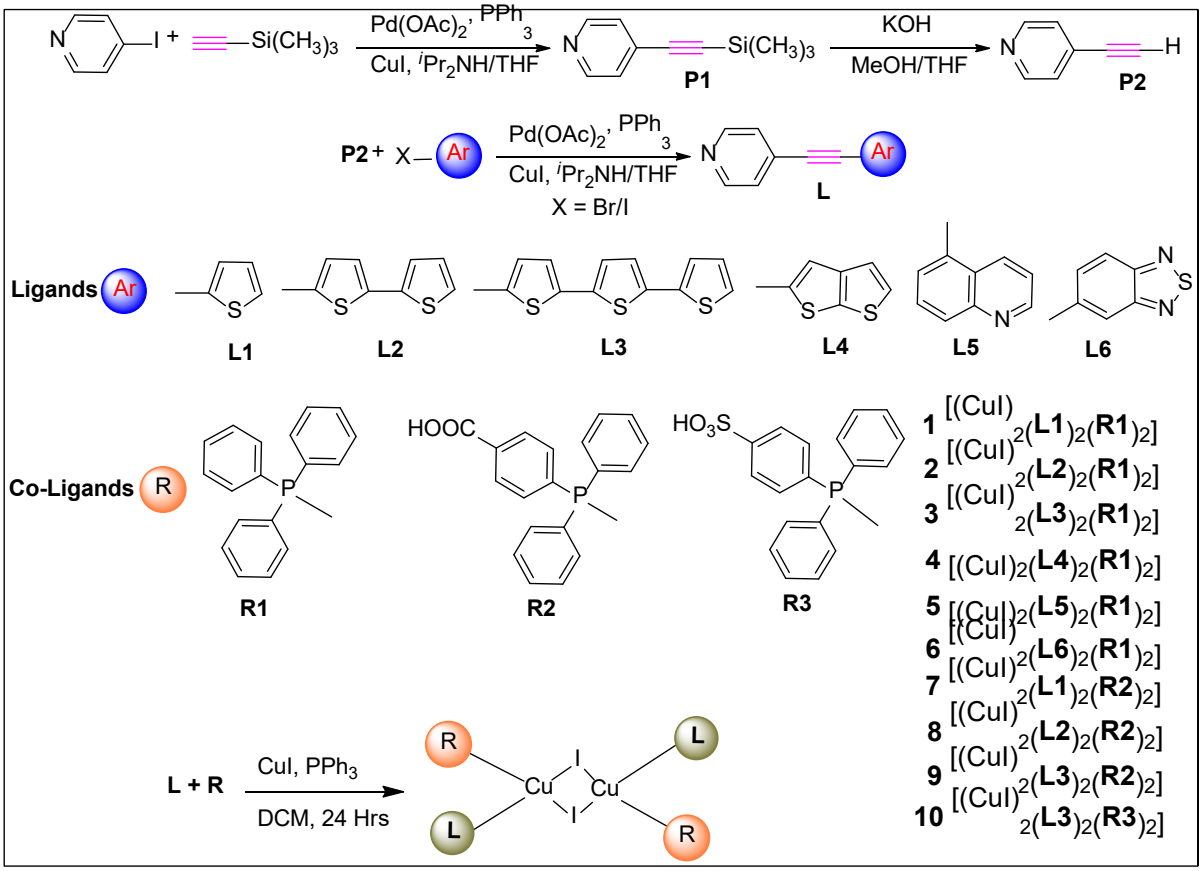

Scheme 1: The synthesis of non-fused and fused heteroaryl ethynylpyridinyl ligands (**L1-L6**) and their corresponding dinuclear Cu(I) complexes **1-10**.

Structural characterization

Spectroscopic results were further complemented by the analysis of the crystal and molecular structures of complexes **1**, **2**, **4**, **5**, and **6 (Figure 1)**. The crystals were grown by slow diffusion of hexane in dichloromethane. Key bond parameter data are summarized in **Table 1**.

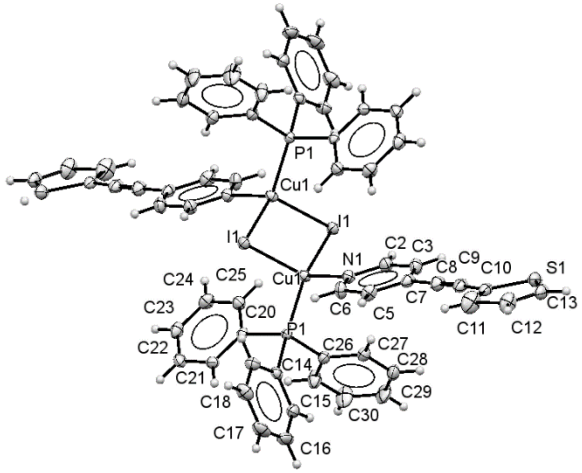

1

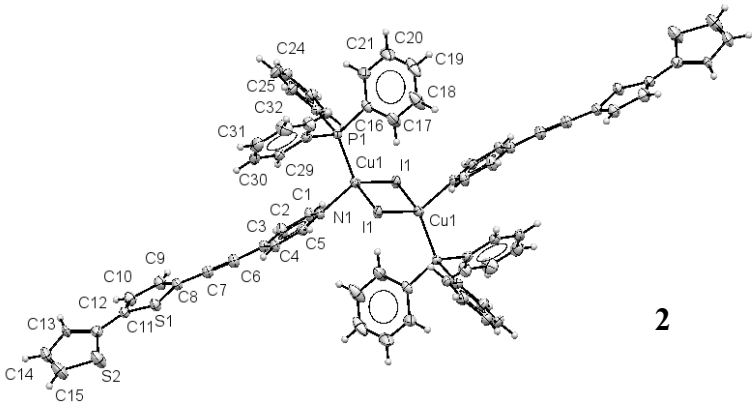

2

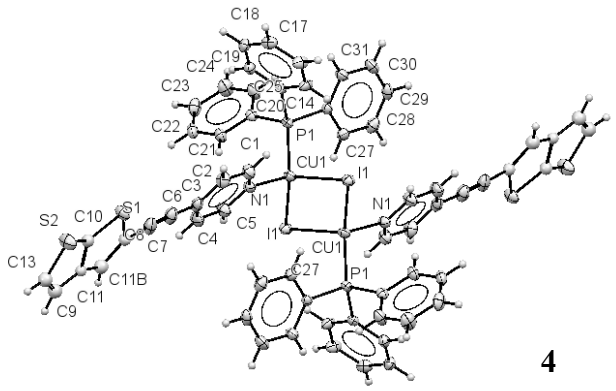
C18
C17
C19
C24
C31
C30
C23
C25
C20
C14
C29
C22
P1
C28
C21
C1
CU1
C27
C2
I1
C3
C6
N1
N1
S2
C10
S1
C5
I1
C8
C7
C4
CU1
C13
C27
P1
C11B
C11
C9

4

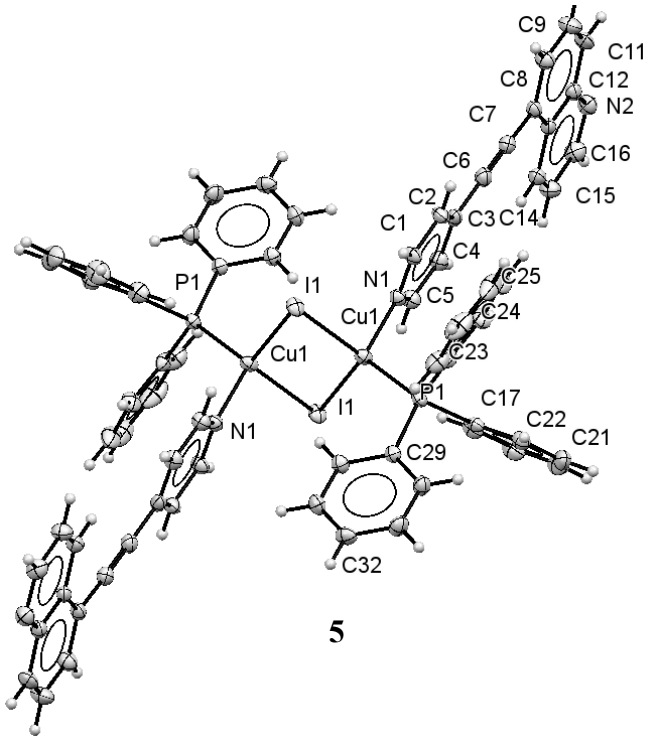
C9
C11
C8
C12
N2
C7
C6
C16
C2
C15
C1
C3
C14
C4
C25
P1
I1
N1
C5
C24
Cu1
Cu1
C23
P1
C17
I1
C22
C21
N1
C29
C32

5

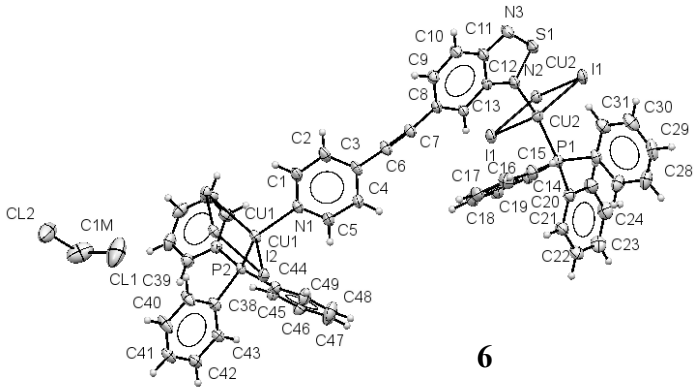

6

Figure 1: The crystal and molecular structures of **1**, **2**, **4**, **5**, and **6** showing the atomic labeling scheme.

As shown in **Figure 1** the crystal structure determinations of the dimeric complexes $[Cu_2I_2(PPh_3)_2(\mathbf{L1})_2]$, $[Cu_2I_2(PPh_3)_2(\mathbf{L2})_2]$, $[Cu_2I_2(PPh_3)_2(\mathbf{L4})_2]$, and $[Cu_2I_2(PPh_3)_2(\mathbf{L5})_2]$ establish that they have a similar Cu_2I_2 core and a *trans* arrangement of the two phosphine and the two **L** ligands. Each Cu(I) center is in a tetrahedral coordination environment consisting of two bridging iodo ligands, one PPh_3 and the nitrogen atom of 4'-pyridinyl substituent of **L1**, **L2**, **L4** or **L5**, respectively. Each molecule sits on a crystallographic center of inversion at the center of the Cu_2I_2 parallelepiped so that there is half a molecule in the asymmetric unit. Within each dimer, the two unique Cu-I distances show a variation between 0.01 and 0.08 Å, with a range from 2.6360(3) to 2.7178(4) Å across the series. The angles at Cu are obtuse with a range of 112.166(1) – 113.967(14)°, while, as required, the angle at the iodine center is acute with a range 66.034(14) – 67.835(10)°, as is observed in other complexes containing a Cu_2I_2 core. The Cu···Cu separations in the dimers show only a small variation from 2.9191(8) to 2.9731(5) Å, which is too long a distance for a formal Cu-Cu bonding interaction. The average Cu–N and Cu–P distances for the series of dimeric complexes are 2.06 Å and 2.21 Å, respectively, and show little variation across the series. Generally, these values for the bond parameters around the Cu(I) center are comparable to those reported previously in other dimeric Cu_2I_2 systems.[12] However, it is apparent that the different coordinating pyridines (**L1, L2**, **L4,**and **L5**) have little effect on the Cu–N bond lengths

suggesting that the differing electronic properties of the ligands do not extend to the environment around the Cu(I) centers.

An examination of the crystal structures of the four dimeric complexes shows that there are no strong intermolecular interactions except in the case of $[Cu_2I_2(PPh_3)_2(\mathbf{L5})_2]$ **5**, where there is a π···π stacking interaction between the quinoline groups on adjacent molecules. The centroid-centroid distance is 3.926 Å and the offset is 1.849 Å. The incorporation of the benzothiadiazole ligand, **L6**, into the copper complex **6** has a major effect on its solid-state structure. The bidentate **L6** acts as a bridging ligand by linking of two Cu_2I_2 cores through pyridine and benzothiadiazole units. This leads to the formation of a 1D polymer with the formula: $[Cu_2I_2(PPh_3)_2(\mathbf{L6})_2]_\infty$. Again, each of the Cu_2I_2 units sits around a crystallographic center of symmetry so that the parallelepipeds are required to be planar. In this instance, there are two independent "Cu_2I_2" in the polymer and they exhibit somewhat different parameters (see Table 1) with the Cu···Cu distance for one of the unique centers being 3.315(2) Å while the other is 2.978(2) Å. This is reflected in the variation in the Cu-I-Cu and I-Cu-I angles which show a difference of *ca*. 3° compared to a difference of only 1° for the dimeric complexes discussed above. Figure 2 shows one strand of the polymer $[Cu_2I_2(PPh_3)_2(\mathbf{L6})_2]_\infty$ which is stabilized through weak π-π interactions between the aromatic rings. S···HC intermolecular interactions of 2.9 Å are also evident. A molecule of dichloromethane of crystallization is also present in the lattice.

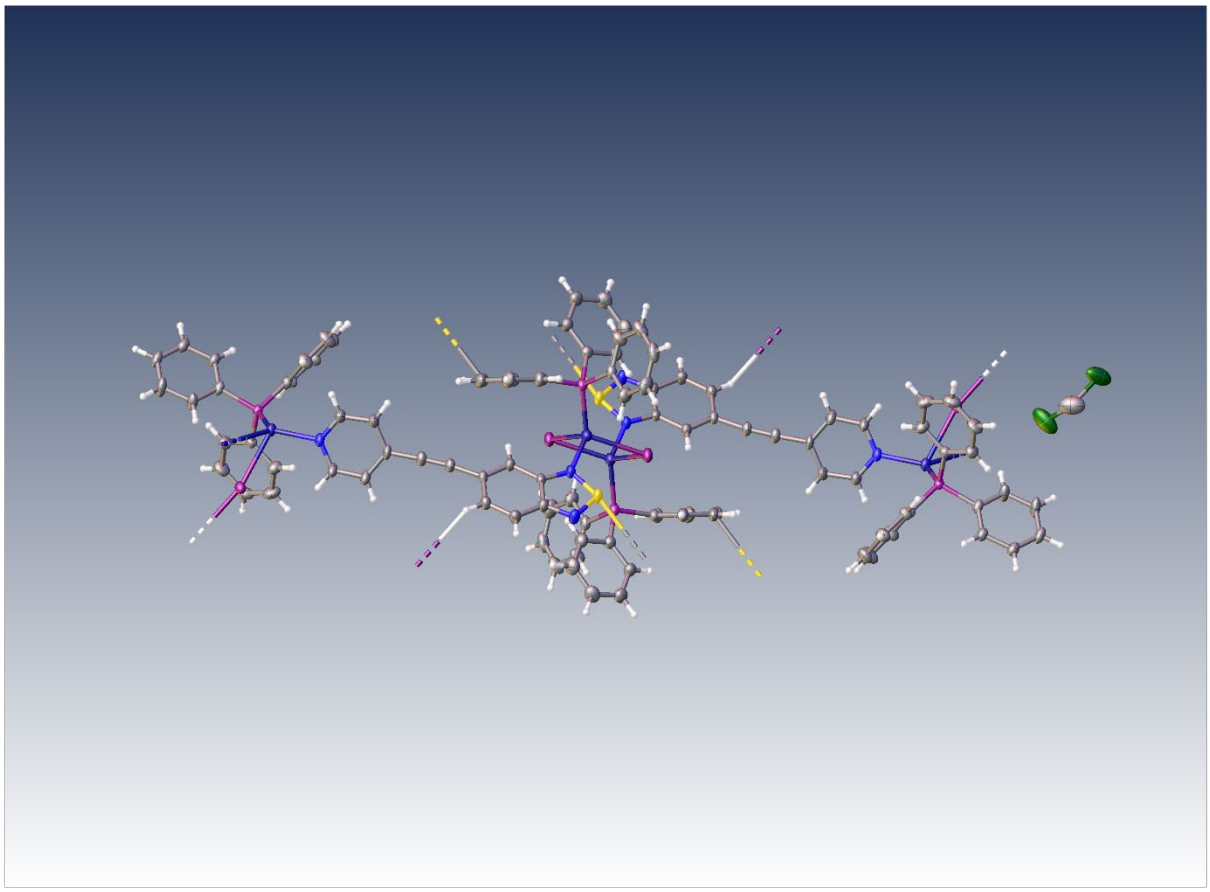

Figure 2: A diagram of one strand of the polymer $[Cu_2I_2(PPh_3)_2(L6)_2]_\infty$, exhibiting weak π-π and S···HC interactions between the aromatic rings.

Table 1: Selected bond parameters for compounds **1**, **2**, **4**, **5** and **6** (Å and °)

	1[(i)]	**2**[(ii)]	**4**[(iii)]	**5**[(iv)]	**6** (Cu dimer 1)[(v)]	**6** (Cu dimer 2)[(v)]
Cu(1)-I(1)	2.6516(3)	2.6381(4)	2.6681(3)	2.6360(3)	2.6832(13)	2.6506(8)
Cu(1)-I(1#)	2.6642(3)	2.7178(4)	2.6552(3)	2.6914(3)	2.6743(9)	2.6412(11)
Cu(1)-P(1)	2.2259(5)	2.2376(7)	2.2251(6)	2.2327(6)	2.2339(13)	2.2179(13)
Cu(1)-N(1)	2.0510(16)	2.060(2)	2.0571(17)	2.0531(18)	2.060(3)	2.052(4)
Cu(1)…Cu(1#)	2.9624(5)	2.9191(8)	2.9680(5)	2.9731(5)	3.315(2)	2.978(2)
Cu(1)-I(1)-Cu(1#)	67.736(10)	66.034(14)	67.771(10)	67.835(10)	71.63(3)	68.48(3)
I(1)-Cu(1)-I(1#)	112.263(9)	113.967(14)	112.230(10)	112.166(10)	108.37(3)	111.52(3)

(i) -x, -y+1, -z+1; (ii) -x+1, -y+2, -z+1; (iii) -x, -y, -z+1 (iv) -x+2, -y, -z-1; (v) -x+1, -y+1, -z

Optical spectroscopy

The electronic spectra of complexes **1-10** were collected in dichloromethane at room temperature (**Figure 3a,b**) and the data are compiled in **Table 2**. As can be seen, all complexes showed a strong high energy (HE) bands with λ_{max} within 300 nm-400 nm attributed to π-π* transition in organic group(s). A trend similar to the variation in IR bands was observed in the UV spectra. Complex **1** having one thienyl ring showed a band at 323 nm (ε = 11 x 10^3 $M^{-1}cm^{-1}$), which shifted significantly to the red (369 nm, ε = 6.8 x 10^3 $M^{-1}cm^{-1}$ and 397 nm ε = 6.2 x 10^3 $M^{-1}cm^{-1}$) for complexes **2** and **3** bearing bithienyl and terthienyl, respectively, essentially due to extended conjugation. In contrast, complex **4** bearing fused the thieno[2,3-*b*]thiophene spacer showed λ_{max} at 331 nm (ε = 5.7 x 10^3 $M^{-1}cm^{-1}$), much lower than its non-fused bithienyl analogue **2**. This can be attributed to the decreased number of double bonds in the fused systems compared to non-fused systems.[27] The onset of absorption for anchored Cu(I) complexes **7**-**10** was found to be red-shifted compared to their PPh_3 analogues (**Table 2**). Another interesting feature was the similarity of band shapes of non-anchored (**1**, **2**, and **3**) complexes with anchored (**7**, **8**, and **9**) counterparts. Similar trend has been observed in the optical band-gaps (E_g^o) of the complexes. These observations were complemented by theoretical calculations (vide-infra).

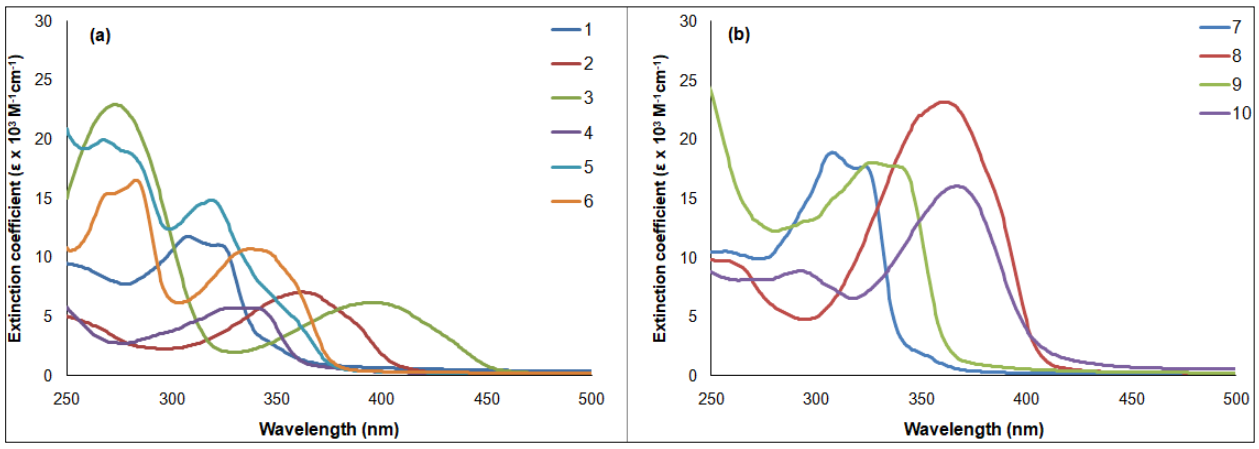

Figure 3: (a) UV-Vis spectra of complexes **1-6** and (b) anchored Cu(I) complexes **7-10**.

Trends similar to those in the IR data were also observed in the PL studies. It has been established that the emission properties of Cu(I) complexes depend on the organic ligands (type, rigidity, and conjugation), the size of the complex as well as Cu···Cu bond distances.[9] Photo-emission of non-anchoring ligand based complexes **1-6** in dichloromethane solution is shown in **Figure 4a**, while for non-anchored ligand based complexes **7-10** are depicted in **Figure 4b**. Almost all complexes exhibited a broad green to blue emission (λ_{em} = 358-486 nm) in solution without any vibronic progression at RT, which is consistent with related Cu(I) complexes.[28] The emission wavelength of the complexes shifted bathochromically on moving from complex **1** (358 nm) through **2** (435 nm) to **3** (479 nm). The nature and extent of shifting unarguably indicated conjugation-directed luminescence control in these complexes.

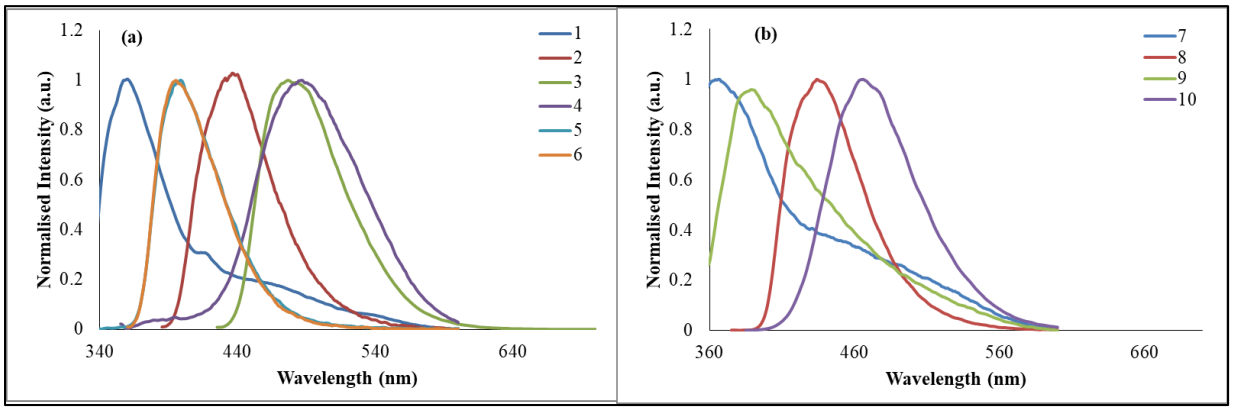

Figure 4: (a) PL spectra of complexes **1-6** and (b) anchored Cu(I) complexes **7-10**.

Table 2: UV-Vis and PL spectral data of complexes **1-10** in dichloromethane at room temperature.

Complex	Absorption profile		Luminescence profile	
	λ_{max}/nm (ε x 10^3 $M^{-1}cm^{-1}$)	Optical band-gap (E_g^o, eV)	λ_{ex} (nm)	λ_{em} (nm)
1	308 (11.7), 323 (11)	3.36	310	358
2	280 (22), 369 (6.8)	2.90	380	435
3	274 (22.9), 397 (6.2)	2.63	420	479
4	331 (5.7)	3.20	350	486
5	269 (19.9), 282 (18.6), 319 (14.9)	3.30	335	398
6	270 (15.4), 284 (16.5), 337 (10.7)	3.03	355	395
7	307 (18.9), 325 (17.5)	2.78	310	368
8	260 (9.6), 362 (23.1)	2.80	370	434
9	326 (18), 341 (17.6)	2.27	345	386
10	293 (8.9), 368 (16)	2.52	380	465

Computational modeling

In order to obtain an insight into the optical spectroscopic results, we performed quantum-chemical calculations using hybrid density functional theory (DFT). The computational methodology is described in detail in the Experimental Section. The optimized geometries of the complexes were obtained at the B3LYP level of theory with the Lanl2dz for iodine and 6-31G(d) for all other atoms (**Figure S1,** *supporting information*). **Figures S2** and **S3** (*supporting information*) depict frontier molecular orbital diagrams and simulated absorption spectra of the complexes, respectively. The Cartesian coordinates of the optimized geometries are provided in **Table ST1** *(supporting information)* while theoretically calculated band gaps (E_g^c, eV) are given in **Table 3**.

The frontier molecular orbitals (HOMOs/LUMOs) together with simulated absorption spectra of two representative examples (complexes **7** and **10**) are shown in **Figure 5 (a-d)**. As expected, HOMO of the complexes was mainly localized over metal center with little contribution of triphenylphosphine co-ligand. On the other hand, LUMO was mainly delocalized over ethynylpyridine-based ligands (**Figure 5a,b**). The main trends in the simulated spectra compare reasonably well with the corresponding solution spectra (**Figure 5c,d**), although simulated spectra show more than one peak for all complexes. For example, complexes **1** and **2** showed λ_{max} at 320

nm and 360 nm, respectively in TD-DFT study (**Figure S3**, *supporting information*), which agrees well with those obtained experimentally (308 nm and 369 nm, respectively, **Figure 3**). Contrarily, complex **3** showed λ_{max} at 315 nm in the TD-DFT calculation (**Figure S3**, *supporting information*), which was found at 397 nm experimentally (**Figure 3**). Similarly, complex **4** showed a λ_{max} at 335 nm (**Figure S3**, *supporting information*), which agrees very well with the experimental value of 331 nm (**Figure 3**). In addition to matching absorption values, simulated spectra also showed the similar trend as the experimental spectra (*viz*. bathochromic shift in absorption peaks with increasing conjugation, i.e. **1** → **3**, **Figure S3**, *supporting information*). The electrical transport properties of a molecule depend on the energy gap between HOMO and LUMO orbitals. It is interesting to note that the values of calculated HOMO-LUMO energy gap, although different (lower) from the experimental one, followed the same trend as experimental ones (**Table 3**). Both the experimental and computational studies showed the lowering of the band gap on moving from complexes **1** → **3**.

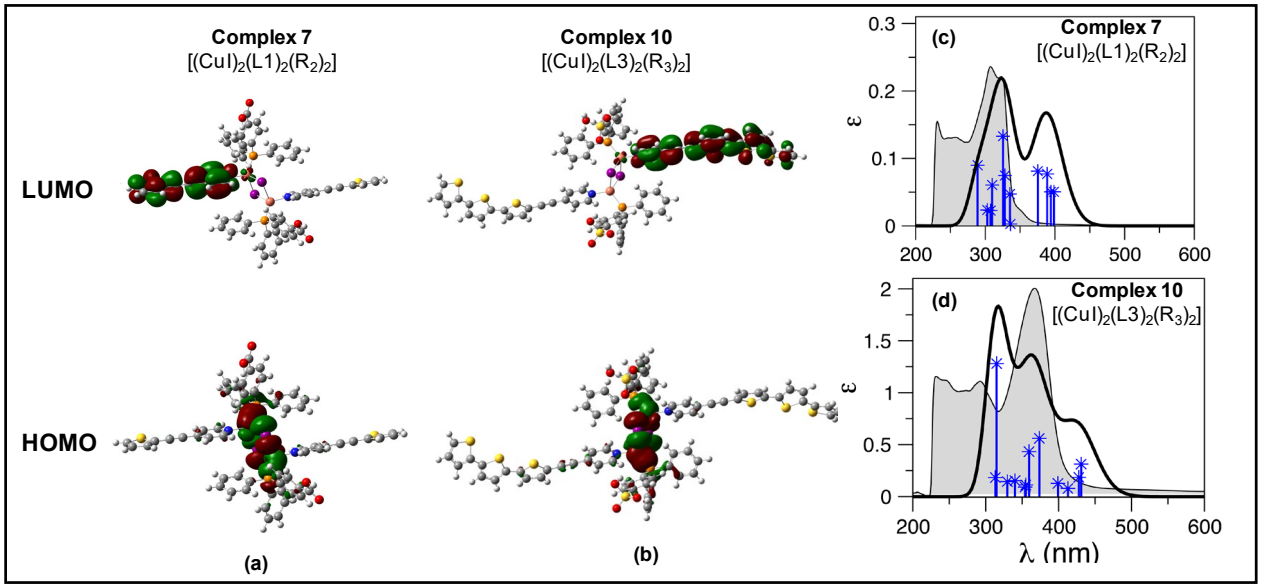

Figure 5: (a & b) Frontier orbitals and (c & d) simulated absorption spectra from TD-DFT calculations in dichloromethane (black line) compared to solution absorption spectra (shaded area) of complexes **7** & **10**. Each plot shows the simulated absorption profile obtained from the spin-allowed singlet states (blue line). These plots were prepared using the GaussView 6 visualization software.[29]

Table 3: Theoretical and experimental values of the frontier molecular orbital energies and band-gaps of the Cu(I) complexes.

Complex	Theoretical[a]			Experimental[b]
	HOMO (eV)	LUMO (eV)	(E_g^c, eV)	(E_g^o, eV)
1.	-4.53	-2.12	2.40	3.36
2.	-4.41	-2.20	2.21	2.90
3.	-4.40	-2.29	2.11	2.63
4.	-4.44	-2.15	2.29	3.20
5.	-4.56	-2.26	2.29	3.30
6.	-4.67	-2.92	1.75	3.03
7.	-4.68	-2.20	2.47	2.78
8.	-4.50	-2.26	2.24	2.80
9.	-4.53	-2.32	2.21	2.27
10.	-4.64	-2.41	2.22	2.52

[a]Energy levels and calculated band-gap (E_g^c, eV) of Cu(I) complexes obtained at the B3LYP/6-31G(d)+Lanl2dz level of theory. [b]Optical band-gap (E_g^o, eV) was calculated from the onset of absorption from dicholoromethane solution spectra using the formula $E_g^o = [1240/\lambda_{onset}]$ (eV).

Electrochemical Studies

Cyclic voltammetry (CV) and differential pulse voltammetry (DPV) data were obtained in anhydrous acetonitrile (ACN) solution to provide complementary information about redox reactivity for metal complexes **1** to **6**. All the materials exhibit oxidation responses (all chemically irreversible) close to 0.9 V vs. $Fc^{0/+}$, which are likely to be associated at least initially with the oxidation of the Cu_2I_2 core. Complex **2-5** showed very similar values of the oxidation potentials (See **Table 4**, DPV data) because of their close HOMO energy levels. Complex **6** showed the highest oxidation potential value of 0.99 V consistent with its HOMO energy level being very low (-4.67 eV). The oxidation potential value of complex **1** and **6** are found to be very similar though there are significant energy difference between their HOMO levels. This is likely to be due to fast and irreversible reaction steps. Due to the limited information that can be extracted from these data and the multi-step character of processes, ligand contributions are possible. In the CV data (**Figure S4**, *supporting information*), all oxidation peak currents are chemically irreversible (without a back-reduction peak in this time domain) and therefore likely to be associated with fast follow-up chemical steps, which may affect both the ligands or the core of the complex. This redox reactivity of the oxidized form of the metal complexes could be relevant to characteristics in DSSCs, as

photo-excitation is likely to lead to electron injection and a period of "hole reactivity" on the metal complex (*vide infra*).

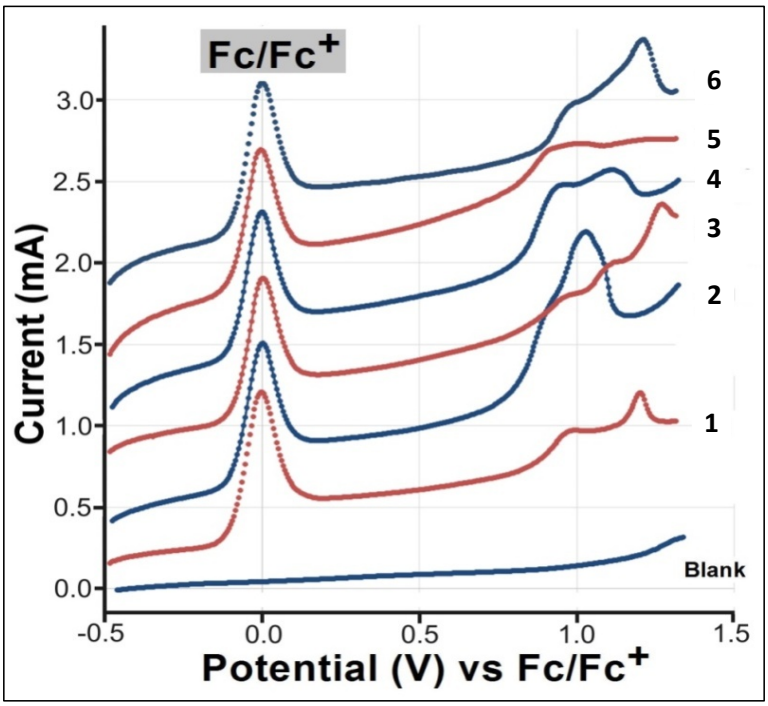

Figure 6: Differential pulse voltammetry (DPV) data (Modulation time = 0.1 s, interval time = 0.5 s and modulation amplitude = 0.05 V) obtained at a 3 mm diameter glassy carbon disc electrode for complexes **1**, **2**, **3**, **4**, **5** and **6** approximately 1 mM in anhydrous ACN with 0.1 M NBu_4PF_6 electrolyte.

Table 4 summarizes the peak potential data. **Figure 6** shows a typical set of differential pulse voltammetry data sets for complexes **1**, **2**, **3**, **4**, **5** and **6**. Complexes **2** and **4** appear to be slightly more sensitive to oxidation but all complexes show activity at approximately 0.9 V vs. $Fc^{+/0}$. A comparison of cyclic voltammetry data and differential pulse voltammetry data suggests similar trends. Oxidation peaks in differential pulse methods are sometimes shifted in potential but there is generally a good correlation.

Table 4: Summary of electrochemical data for Cu(I) complexes **1-6**.

Materials	**Cyclic voltammetry(CV)** $E_{ox,peak}$ **(V vs.** $Fc^{0/+}$**)**	**Differential pulse voltammetry (DPV)** $E_{ox,peak}$ **(V vs.** $Fc^{0/+}$**)**
1	0.94, 1.17	0.98, 1.20

2	0.96, 1.13	0.91, 1.03, 1.09
3	0.96, 1.08, 1.24	0.96, 1.10, 1.27
4	0.99, 1.09	0.95, 1.12
5	0.99	0.90, 1.01
6	0.96, 1.17	0.99, 1.21

Photo-voltaic performance

To underpin the PV performance of the developed materials, we have fabricated DSSCs of complexes **7**-**10** (bearing anchoring groups). The TiO_2 photo-anodes based on different dyes were used to assemble DSSCs with platinized counter electrodes and a classical I^-/I_3^- based redox couple. Although low in efficiency, devices showed performances comparable to many other homoleptic Cu(I)-based DSSCs.[3] **Figure 7a** shows that the current density-voltage (*J-V*) curves of the DSSCs measured under irradiation of AM1.5 simulated solar light (100 $mWcm^{-2}$), and the corresponding parameters are summarized in **Table 5**. TiO_2 films with **10** based device showed the highest photoelectric conversion efficiency (PCE = 1.56%), with improved V_{oc}= 0.52 V, J_{sc} = 4.43 mA/cm^2, and FF = 69%. To the contrary, the DSSCs based on the dye **7** showed the lowest photovoltaic performance (PCE = 0.15%) with V_{oc} of 0.41 V, J_{sc} = 0.53 mA/cm^2, and FF = 68%. Complex **7** has lower PCE than the reported[30] thiophene-functionalized 2,2′-bipyridine incorporated Cu(I) complex bearing carboxylic acid anchoring group (**C1**), which showed a PCE of 1.16%. Similarly, **C1** showed better SC performance compared to the Cu(I) complex having no thiophene moiety.[12] This can be attributed to the bathochromic shift of MLCT band and a higher HOMO energy level of **C1**, which suggest that the SC performance can be improved by incorporating the thiophene moiety into the ligand. For example, V_{oc}, J_{sc}, FF, and PCE rise on going from **7**→**9**, which can be attributed to increasing number of thienyl units attached to pyridine. As reported in other studies[3], we also noted that complex bearing carboxyl functionality as an anchoring unit showed inferior performance compared to the sulfonated analogue. A sudden rise in the performance on using complex **10** can be attributed to synergistic effect of terthiophene spacer in combination with anchoring group. For an efficient electron transfer between the sensitizer, the semiconductor, and the electrolyte, it is important to match energy levels (HOMO and LUMO) of the complexes with the conduction band of TiO_2 and redox potential of the electrolyte. We found that LUMO orbital (-2.20 eV, -2.26 eV, -2.32 eV, -2.41 eV for **7**, **8**, **9**, and **10**, respectively, **Table 3**) was above the conduction band of TiO_2 (E_{CB} = -4.0 eV).[31] Interestingly, the gap between LUMO and E_{CB} follows the order: **7** (1.80 eV), **8** (1.74 eV) > **9** (1.68 eV) > **10** (1.59 eV), providing enough power for electron injection (> 0.3 eV).[32] Close HOMO energy level

of **10** (-4.64 eV) with redox potential of the electrolyte (I^-/I_3^- = -4.80 eV)[31] might have also contributed. For the complexes **9** and **10** with **L3**, **10** has a higher dye regeneration power of 4.16 eV (-4.80 eV HOMO), which is beneficial to the improvement of its PCE and suppression of electronic recombination. Furthermore, higher light to energy conversion by complex **10** may also be linked to its absorption profile, which was most bathochromically shifted. The IPCE values of DSSCs based on **10** are higher than those of other dyes from 300 nm to 800 nm (**Figure 7b**). The IPCE values of **10** are above 50% within a wider range of wavelengths, which demonstrates that **10** is a better photosensitizer for DSSCs. Consequently, DSSC based **10** dye has more efficient charge collection efficiency than other dyes. This fact is further supported by higher short current density (J_{sc}) obtained from the J-V curves. Compared to other Cu(I)–based complexes[31], our homoleptic systems demonstrated lower performance. Since there are several compositional and device related factors that control overall performance of the device, it would be too early to blame any single factor for overall low device performance. However, we attribute comparatively low performance to increased rigidity (and thus enhanced the π-π interaction) of the molecule, leading to the formation of aggregates of the dyes on the surface of TiO_2.

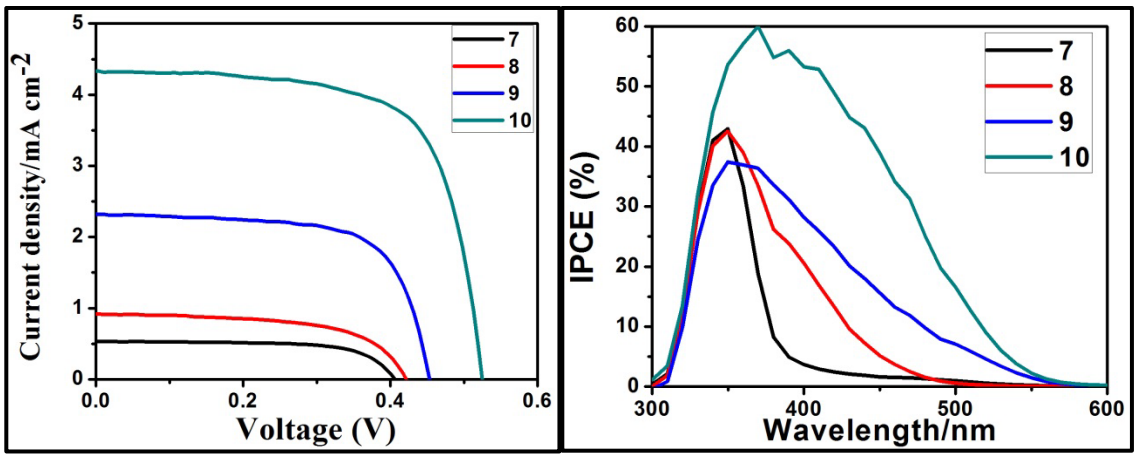

Figure 7: (a) J-V curves and (b) IPCE spectra for DSSCs based on different dyes with I^-/I_3^- redox electrolyte.

Table 5: Photovoltaic parameters of DSSCs based on different dyes under an illumination of 100 mW cm^{-2}, AM 1.5 G condition.

Device	V_{oc} (V)	J_{sc}(mA cm^{-2})	FF (%)	PCE (%)	IPCE (%)
7	0.41	0.53	68	0.15	42.05
8	0.42	0.92	60	0.23	42.51
9	0.45	2.32	68	0.72	37.53

10	0.52	4.43	69	1.56	58.14
C1 (Ref.[30])	0.55	2.95	71	1.16	14-17

CONCLUSION

A series of new neutral Cu(I) complexes **1**-**10** of non-fused/fused heteroarylethynylpyridinyl-ligands (**L**) with CuI and the co-ligand including PPh_3 (**R1**) or anchored $PPh_2(C_6H_4COOH)$/ $PPh_2(C_6H_4SO_3H)$ (**R2**/ **R3**) have been synthesized. The absorption was found to be red-shifted with the presence of an increasing number of thienyl units in complexes **1**-**3** whereas the onset absorption of complex **4** was found to be blue-shifted compared to the complex **2** which may be attributed to a reduced number of double bonds in the fused system. The absorption of anchored Cu complexes **7**-**10** was found to be red-shifted in comparison with complexes **1**-**6**. Rhomboid dimeric structures for complexes **1**, **2**,**4** and **5** and polymeric structure for **6** have been established by single crystal X-ray structure analysis. All the complexes exhibit oxidation potential responses close to 0.9 V vs. $Fc^{0/+}$ which are associated with follow-up chemical and electrochemical reaction steps. The anchored Cu-complexes **7**-**10** displayed PCE in the range of 0.15-1.56% in DSSCs. Complex **10** containing the sulfonic acid functionality showed the highest PCE of 1.56%. The structures of all the Cu complexes have been optimized, and their HOMO and LUMO energy levels have been determined by DFT and TD-DFT calculations. The LUMO energy level of dye materials was found to be higher than that of the conduction band of the TiO_2, which facilitated effective electron transport. Theoretical calculations have complemented the optical absorption and photovoltaic characteristics of these complexes.

EXPERIMENTAL SECTION

General procedures

All reactions were performed under a dry argon atmosphere using the standard Schlenk line technique. Solvents were pre-dried and distilled before use by standard procedures.[13] All chemicals, except where stated otherwise, were obtained from Sigma-Aldrich and TCI Chemicals and used as received. The key starting material 4-(trimethylsilylethynyl)pyridine (**P1**) and 4-ethynylpyridine (**P2)** were synthesized by adaptation of the literature method.[33] Elemental analyses were performed in the microanalysis laboratory of the Department of Chemistry, University of Cambridge, UK. NMR spectra were recorded in $CDCl_3$ using a Bruker Advance III HD 700 MHz

spectrometer equipped with 5 mm TCI H/C/N cryoprobe. The ^{1}H and ^{13}C NMR spectra were referenced to solvent resonances and $^{31}P\{^{1}H\}$ NMR spectra were referenced to external phosphoric acid. IR spectra were recorded directly on the sample as attenuated total reflectance (ATR) on Diamond using Cary 630 FT-IR spectrometer. UV/Vis spectra were recorded with an Agilent Cary 5000 UV-visible spectrophotometer using a quartz cuvette with a 1 cm path length. Mass spectra were acquired using a Kratos MS 890 spectrometer using electron-impact (EI) and electrospray-ionization (ESI) techniques. Preparative thin-layer chromatography was carried out on commercial Merck plates with a 0.25 mm layer of silica. Column chromatography was performed using silica gel (230-400 mesh).

Caution! All chemicals used in the current work are irritants to skin, eyes and the respiratory system. Therefore, all reactions were performed in a well-ventilated fume hood. Inhalation of silica/alumina and low boiling point solvents like dichloromethane and hexane may cause injuries to internal organs. Safety glasses, gloves, masks and lab coats were worn during the experiments.

Ligand synthesis

4-(Trimethylsilylethynyl)pyridine, **P1**

To a solution of 4-iodopyridine (4 g, 19.51 mmol) in $^{i}Pr_2NH$/THF (150 cm^3, 1:4 v/v) were added catalytic amounts of $Pd(OAc)_2$ (44 mg), CuI (46 mg), and PPh_3 (256 mg) under an Ar atmosphere. After stirring for 30 min, trimethylsilylacetylene(3.3 mL, 23.41 mmol) was added dropwise followed by overnight reflux. The completion of the reaction was confirmed by silica TLC and IR spectroscopy. The reaction mixture was concentrated under reduced pressure and the crude residue was subjected to silica gel column chromatography using hexane/CH_2Cl_2 (1:1, v/v) as eluent to yield the title compound as an orange oil (3.05 g, 89 %). IR (ATR, diamond):ν/cm^{-1} 2165 (–C≡C–). ^{1}H NMR: δ/ppm 7.28 (d, J = 5.0 Hz, 2H, $H_{\beta\text{-pyr}}$), 7.22 (d, J = 5.0 Hz, 2H, $H_{\alpha\text{-pyr}}$), 0.27 (s, 9H, $SiMe_3$).^{13}C NMR (700 MHz, $CDCl_3$, ppm):δ/ppm 150. 29, 126.41, 128.79, (Aromatic C) 90.63, 89.21 (–C≡C–), 0.15 (C of $Si(CH_3)_3$). ESI-MS m/z 175.30. Anal. Calc. for $C_{10}H_{13}NSi$: C, 68.51; H, 7.47; N, 7.99%; found: C, 68.53; H, 7.45, N, 7.97%.

4-Ethynylpyridine, **P2**

P1 (3.0 g, 17.11 mmol) was proto-desilylated in THF/methanol (20 mL, 4:1, v/v) using aqueous KOH (1.92 g, 34.21 mmol). The reaction mixture was stirred at room temperature for 1.5 h. during which time TLC and IR revealed that all protected compound has been converted to the terminal alkyne ligand. The solvent mixture was then removed and the residue was dissolved in a small

amount of CH_2Cl_2 and subjected to column chromatography on silica using hexane/CH_2Cl_2(1:1, v/v) as eluent to give 4-ethynylpyridine as an off-white solid (1.52 g, 86%). IR (ATR, diamond): ν/cm^{-1}: 3223 ($\nu_{(R\text{-}C\equiv C\text{-}H)}$) and 2109 ($\nu_{(R\text{-}C\equiv C\text{-})}$).^{1}H NMR (700 MHz, $CDCl_3$, ppm): δ/ppm 7.55 (d, *J* = 6.0 Hz, 2H, $H_{\beta\text{-pyr}}$), 7.40 (d, *J* = 5.4 Hz, 2H, $H_{\alpha\text{-pyr}}$), and 4.00 (s, 1H, C≡C-**H**). ^{13}C NMR (700 MHz, $CDCl_3$, ppm): δ/ppm 132.3, 128.4, 128.3, 122.7 (Aromatic C), 89.6, 85.4(–C≡C–). ESI-MS: m/z X 103.09. Anal. Calc. for C_7H_5N: C, 81.53; H, 4.89; N, 13.58%; found: C, 81.59; H, 4.86; N, 13.61%.

4-(Thiophene-2-ylethynyl)pyridine, **L1**

To a solution of 4-ethynylpyridine, **P1** (0.12 g, 1.16 mmol) in ^{i}Pr$_2$NH/THF (120 cm^3, 1:4 v/v) under an Ar atmosphere were added catalytic amounts of $Pd(OAc)_2$ (26 mg), CuI (27 mg), and PPh_3 (15.2 mg). The solution was stirred for 0.5 hour and 2-iodothiophene (0.24 g, 1.16 mmol) was added. The reaction mixture was allowed to stir at reflux overnight at ~70°C. Silica TLC and IR spectroscopy were performed from time to time in order to follow the completion of the reaction. After drying the reaction mixture under *vacuum*, the crude residue was subjected to a silica gel column chromatography using hexane/CH_2Cl_2 (2:8, v/v) to afford **L1** as a yellow solid (0.18 g, 84%, m.p. 125.9 ºC). IR (ATR, diamond): ν/cm^{-1} 2203 $\nu_{(–C\equiv C–)}$. ^{1}H NMR (700 MHz, $CDCl_3$):δ/ppm 7.68 (d, *J* = 7.00 Hz, 2H,$H_{\alpha\text{-pyr}}$,), 7.65 (d, *J* = 7.00 Hz, 2H, $H_{\beta\text{-pyr}}$), 7.38 (d, *J* = 1.12 Hz, 1H), 7.35 (d, *J* = 1.12 Hz, 1H), 7.47 (d, *J* = 2.8 Hz,1H).^{13}C NMR (700 MHz, $CDCl_3$, ppm): δ/ppm 149.92, 125.53, 128.87 (C's of pyridine), 122.08, 132.08, 127.49, 127.72 (C of thiophene), 90.53, 87.64 (–C≡C–). ESI-MS: m/z 285.00. Anal. Calc. for $C_{11}H_7NS$: C, 71.32; H, 3.81; N, 7.52%; found: C, 71.42; H, 3.83; N, 7.55%.

4-([2,2'-Bithiophene]-5-ylethynyl)pyridine, **L2**

This compound was synthesized following the procedure described for **L1** using 5-bromo-2,2'-bithiophene (0.26 g, 1.06 mmol).The compound **L2** was obtained as a brownish yellow solid (0.20 g, 71%). IR (ATR, diamond): ν/cm^{-1} 2197 (–C≡C–). ^{1}H NMR (700 MHz, $CDCl_3$): δ/ppm 7.28 (dd, *J* = 1.1 Hz, 2H, $H_{\alpha\text{-pyr}}$), 7.27 (d, *J* = 1.3 Hz, 2H, $H_{\beta\text{-pyr}}$), 7.23 (d, *J* = 3. 57 Hz, 1H), 7.10 (d, *J* = 3.85 Hz,1H), 7.04 (t, *J* = 7.0 Hz, 1H). ^{13}C NMR (700 MHz, $CDCl_3$):δ/ppm149.78, 140.45, 136.37, 134.19, 131.02, 128.06, 125.48, 125.09, 124.65, 123.68, 120.39 (Aromatic C), 91.41, 87.37 (–C≡C–).ESI-MS: m/z 267.9. Anal. Calc. for $C_{15}H_9NS_2$: C, 67.38; H, 3.39; N, 5.24%; found: C, 67.43; H, 3.41; N, 5.25%.

4-([2,2':5',2''-Terthiophene]-5-ylethynyl)pyridine, **L3**

This compound was synthesized following the procedure described for **L1** using 5-bromo-2,2':5',5"-terthiophene (0.28 g, 0.86 mmol).The compound **L3** was obtained as a dark yellow solid (0.27 g, 90%). IR (ATR, diamond): ν/cm^{-1} 2194 (–C≡C–). ^{1}H NMR 7.36 (dd, *J* = 8.1, 1.5 Hz, 1H), 7.24 (d, *J* = 0.42 Hz, 1H), 7.20 (d, *J* = 1.1 Hz, 1H), 7.19 (d, *J* = 1.1 Hz, 1H), 7.13 (d, *J*=3.7 Hz, 2H), 7.11 (d, *J*=5.2 Hz, 2H), 7.09 (d, *J* = 3.8 Hz, 2H), 7.04 (d, *J* = 3.6 Hz, 1H).^{13}C NMR (700 MHz, $CDCl_3$):δ/ppm 149.87, 140.28, 137.57, 136.88, 135.12, 134.43, 131.21, 128.13, 124.60, 124.40, 124.21, 124.23, 124.09, 123.69, 120.54 (Aromatic C), 91.79, 87.58 (–C≡C–). ESI-MS: m/z 347.8. Anal. Calc. for $C_{19}H_{11}NS_3$: C, 65.30; H, 3.17; N, 4.01%;found: C, 65.43; H, 3.19; N, 4.05%.

4-(Thieno[2,3-b]thiophen-2-ylethynyl)pyridine, **L4**

This compound was synthesized following the procedure described for **L1** using 2-bromothieno[3,2-b]thiophene (0.21 g, 0.96 mmol). The compound **L4** was obtained as a yellow solid (0.19 g, 86%). IR (ATR, diamond): ν/cm^{-1} 2198 (–C≡C–). ^{1}H NMR (700 MHz, $CDCl_3$):δ/ppm 7.69 (dd, *J* = 3.8, 1.3 Hz, 2H), 7.68 (t, *J* = 1.6 Hz, 2H), 7.57 – 7.56 (m, 1H), 7.55 (dd, *J* = 2.8, 1.4 Hz, 1H), 7.28 (s, 1H). ^{13}C NMR (700 MHz, $CDCl_3$):δ/ppm 145.89, 139.42, 132.25, 131.97, 129.17, 128.56, 125.87, 124.37, 120.03(Aromatic C), 90.94, 87.72 (–C≡C–). ESI-MS: 241.9. Anal. Calc. for $C_{13}H_7NS_2$: C, 64.70; H, 2.92; N, 5.80%; found: C, 64.63; H, 2.88; N, 5.85%.

5-(Pyridin-4-ylethynyl)quinoline, **L5**

This compound was synthesized by adapting the procedure described for **L1** using 5-bromoqinoline (0.2 g, 0.96 mmol). The compound **L5** was obtained as a yellow solid (0.18 g, 81% yield). IR (ATR, diamond): ν/cm^{-1} 2217 (–C≡C–). ^{1}H NMR (700 MHz, $CDCl_3$): δ/ppm 8.59 (d, *J = 8.3 Hz,* 2H, $H_{\alpha\text{-pyr}}$), 8.11 (d, *J* = 8.4 Hz, 2H, $H_{\beta\text{-pyr}}$), 7.35-7.78 (m, 6H, Aromatic H).^{13}C NMR (700 MHz, $CDCl_3$): δ/ppm 151.02, 149.69, 147.85, 131.42, 130.92, 128.92, 128.72, 128.50, 128.48, 126.39, 122.01, 120.01 (Aromatic C), 91.99, 80.25 (–C≡C–). ESI-MS: 230.9. Anal. Calc. for $C_{16}H_{10}N_2$: C, 83.46; H, 4.38; N, 12.17%; found: C, 83.63; H, 4.31; N, 12.21%.

5-(Pyridin-4-ylethynyl)benzo[c][1,2,5]thiadiazole, **L6**

This compound was synthesized by adapting the procedure described for **L1** using 5-bromobenzo[c][1,2,5]thiadiazole (0.15 g, 0.70 mmol). The compound was obtained as a yellow solid (0.14 g, 84%, yield). IR (ATR, diamond): ν/cm^{-1} 2215 (–C≡C–).^{1}H NMR (700 MHz, $CDCl_3$): δ/ppm 8.21 (d, *J* = 1.4 Hz, 2H), 7.99 (d, *J = 1.4 Hz*, 1H), 7.67 (d, *J = 1.5 Hz* 2H), 7.44

(br s, 1H), 7.26 (s, 1H).^{13}C NMR (700 MHz, $CDCl_3$): δ/ppm 154.56, 154.47, 149.93, 132.68, 128.58, 126.13, 125.29, 123.63, 121.78 (Aromatic C), 92.63, 89.80 (–C≡C–). ESI-MS: 236.59. Anal. Calc. for $C_{13}H_7N_3S$: C, 65.80; H, 2.97; N, 17.71%; found: C, 65.63; H, 2.87; N, 17.75%.

Synthesis of Cu(I) Complexes

***[(L1)$_2$(CuI)$_2$(PPh$_3$)$_2$],* 1**

Cu(I) complexes were prepared by adapting the recently reported literature method.[19] The ligand **L1** (0.1 g, 0.54 mmol) dissolved in 10 mL of degassed dichloromethane (CH_2Cl_2) was added to a solution of CuI (102 mg) and triphenylphosphine (142 mg) in 15 mL CH_2Cl_2. The mixture was allowed to stir for 24 h at room temperature. The crude product obtained on the removal of solvent under reduced pressure was redissolved in CH_2Cl_2 and passed through plug of celite. Finally, the solvent was removed under reduced pressure to afford **1** as a dark yellow solid (0.25 g, 73%). IR (ATR, diamond): ν/cm^{-1} 2199 (–C≡C–). ^{1}H NMR (700 MHz, $CDCl_3$): δ/ppm 7.76 (dd, , J = 3.2 Hz, 1.9 Hz, 4H, $H_{\alpha\text{-pyr}}$), 7.66-7.40 (m, 34H, P*Ph*$_3$, $H_{\beta\text{-pyr}}$), 7.48 (d, , J = 1.5 Hz, 2H), 7.37 (dd, , J = 1.1 Hz, 2H), 7.35 (d, , J = 1.1 Hz, 2H). ^{13}C NMR (700 MHz, $CDCl_3$):δ/ppm 150.16, 135.39, 134.33, 134.25, 132.94, 131.63, 130.38, 128.69, 127.79, 127.76, 122.01 (Aromatic C), 90.48, 88.12 (–C≡C–). ^{31}P NMR (121.53 MHz, $CDCl_3$): δ = 29.10 (s, P*Ph*$_3$) ppm. ESI-MS: m/z 1227.0. Anal. Calc. for $C_{58}H_{44}Cu_2I_2N_2P_2S_2$: C, 54.60; H, 3.48; N, 2.20%; found: C, 54.63; H, 3.53; N, 2.25%.

***[(L2)$_2$(CuI)$_2$(PPh$_3$)$_2$],* 2**

This compound was synthesized by following a procedure similar to that described above for **1** using **L2** (0.15 g, 0.56 mmol), CuI (107 mg), and triphenylphosphine (147 mg) yielding **2** as a dark yellow solid (0.27 g, 67%). IR (ATR, diamond): ν/cm^{-1} 2199 (–C≡C–). ^{1}H NMR (700 MHz, $CDCl_3$): δ/ppm 8.36 (d, J = 6.1 Hz, 4H, $H_{\alpha\text{-pyr}}$), 7.80-7.38 (m, 34H, P*Ph*$_3$, $H_{\beta\text{-pyr}}$), 7.28-7.32 (m, 6H), 7.05 (d, J = 5.6 Hz, 4H). NMR ^{13}C NMR (700 MHz, $CDCl_3$):δ/ppm 150.22, 141.43, 136.44, 134.52, 132.90, 131.96, 129.64, 128.76, 127.64, 126.28, 125.08 (Aromatic C), 123.83, 124.82 (–C≡C–). ^{31}PNMR (121.53 MHz, $CDCl_3$): δ = 29.10 (s, P*Ph*$_3$) ppm. ESI-MS: m/z 1332.3. Anal. Calc. for $C_{66}H_{48}Cu_2I_2N_2P_2S_4$: C, 55.04; H, 3.36; N, 17.62%; found: C, 65.63; H, 2.87; N, 17.75%.

***[(L3)$_2$(CuI)$_2$(PPh$_3$)$_2$],* 3**

This compound was synthesized by following a procedure similar to that described above for **1** using **L3** (0.17g, 0.49 mmol), CuI (92 mg), and triphenylphosphine (127 mg), yielding **3** as an

orange solid (0.25 g, 63%) IR (ATR, diamond): ν/cm^{-1} 2195 (–C≡C–). ^{1}H NMR (700 MHz, $CDCl_3$): δ/ppm 8.63 (dd, *J* = 4.4, 1.6 Hz, 4H), 7.71 – 7.37 (m, 34H, P*Ph*$_3$, H_{py}), 7.22 (dd, *J* = 3.6, 1.1 Hz, 4H), 7.15 (d, *J* = 3.8 Hz, 4H), 7.12 (dd, *J*= 7.0, 3.8 Hz, 4H), 7.06 (dd, *J* = 5.1, 3.6 Hz, 2H).^{13}C NMR (700 MHz, $CDCl_3$):δ/ppm 149.89, 149.84, 140.16, 137.44, 136.75, 134.99, 134.30, 132.85, 132.26, 132.15, 132.09, 131.96, 131.94, 131.07, 128.55, 128.48, 128.00, 125.27, 125.08, 124.96, 124.47, 124.11, 123.56, 120.41 (Aromatic C), 91.66, 87.47 (–C≡C–). ^{31}PNMR (121.53 MHz, $CDCl_3$): δ = 29.24 (s, P*Ph*$_3$) ppm. ESI-MS: m/z 1532.5. Anal. Calc. for $C_{74}H_{52}Cu_2I_2N_2P_2S_6$: C, 55.40; H, 3.27; N, 1.75%; found: C, 55.53; H, 3.33; N, 1.78%.

***[(L4)$_2$(CuI)$_2$(PPh$_3$)$_2$],* 4**

This compound was synthesized by following a procedure similar to that described above for **1** using **L4** (0.10g, 0.41 mmol), CuI (78mg), and triphenylphosphine (108 mg), yielding **4** as a pale yellow solid (0.20 g, 69%) IR (ATR, diamond): ν/cm^{-1} 2196 (–C≡C–). ^{1}H NMR (700 MHz, CDCl3): δ/ppm 7.90 (m, 4H, $H_{\alpha\text{-pyr}}$), 7.67-7.49 (m, 34H, P*Ph*$_3$, $H_{\beta\text{-pyr}}$), 7.36 (dd, *J* = 4.55 Hz, 2.9 Hz, 2H), 7.23 (d, *J* = 7.0 Hz, 4H). ^{13}C NMR (700 MHz, $CDCl_3$):δ/ppm149.93, 145.87, 145.87, 139.50, 134.11, 134.03, 132.86, 132.68, 132.22, 132.13, 132.96, 131.96, 131.94, 131.11, 129.76, 129.17, 128.55, 128.48, 125.96, 125.22, 124.22, 120.02 (Aromatic C), 90.68, 88.11 (–C≡C–).^{31}P NMR (121.53 MHz, $CDCl_3$): δ = 29.09 (s, P*Ph*$_3$) ppm. ESI-MS: m/z 1385.27. Anal. Calc. for $C_{62}H_{44}Cu_2I_2N_2P_2S_4$: C, 53.64; H, 3.19; N, 2.02%; found: C, 53.54; H, 3.23; N, 2.0%.

***[(L5)$_2$(CuI)$_2$(PPh$_3$)$_2$],* 5**

This compound was synthesized by following a procedure similar to that described above for **1** using **L3** (100 mg, 0.43 mmol), CuI (83 mg), and triphenylphosphine (113 mg), yielding a pale yellow solid (0.19 g, 65%). IR (ATR, diamond): ν/cm^{-1} 2220 (–C≡C–). ^{1}H NMR (700 MHz, $CDCl_3$): δ/ppm 7.86 (d, *J* = 1.1 Hz, 4H, $H_{\alpha\text{-pyr}}$), 7.76-7.46 (m, 34H, P*Ph*$_3$, $H_{\beta\text{-pyr}}$), 7.20-7.10 (m, 12H, Aromatic H). ^{13}C NMR (700 MHz, $CDCl_3$): δ/ppm 151.16, 150.08, 147.92, 134.25, 134.13, 134.05, 132.83, 132.24, 132.14, 132.09, 131.96, 131.94, 131.50, 131.42, 131.22, 129.76, 128.95, 128.55, 128.53, 128.48, 126.19, 125.69, 122.05, 119.99 (Aromatic C), 91.86, 90.94 (–C≡C–).^{31}PNMR (121.53 MHz, $CDCl_3$): δ = 29.14 (s, P*Ph*$_3$) ppm. ESI-MS: m/z 1321.30. Anal. Calc. for $C_{68}H_{50}Cu_2I_2N_4P_2$: C, 59.79; H, 3.69; N, 4.10%; found: C, 59.73; H, 3.63; N, 4.18%.

***[(L6)$_2$(CuI)$_2$(PPh$_3$)$_2$]$_\infty$,* 6**

This compound was synthesized by following a procedure similar to that described above for **1** using **L3** (90 mg, 0.38 mmol), CuI (78 mg), and triphenylphosphine (125 mg), yielding a pale

yellow solid (0.16 g, 61%). IR (ATR, diamond): ν/cm^{-1} 2216 (–C≡C–). ^{1}H NMR (700 MHz, $CDCl_3$): δ/ppm8.66-8.75 (m, 2H, $H_{\alpha\text{-pyr}}$), 8.20-8.29 (m, 1H, $H_{\alpha\text{-pyr}}$), 7.99-8.04 (m, 1H, $H_{\alpha\text{-pyr}}$), 7.66-7.38 (m, 34H, P*Ph*$_3$, $H_{\beta\text{-pyr}}$), 7.17-7.08 (m, 2H), 7.42-7.45 (m, 4H). ^{13}C NMR (700 MHz, $CDCl_3$): δ/ppm154.61, 154.49, 150.29, 134.29, 134.21, 129.83, 128.62, 128.56, 125.91, 121.85 (Aromatic C), 93.13, 89.65 (–C≡C–).^{31}PNMR (121.53 MHz, $CDCl_3$): δ = 29.14 (s, P*Ph*$_3$) ppm. ESI-MS: m/z 1376.2. Anal. Calc. for $(C_{62}H_{44}Cu_2I_2N_6P_2S_2)_\infty$:C, 53.96; H, 3.21; N, 6.09%; found: C, 54.03; H, 3.23; N, 6.12%.

***[(CuI)$_2$(L1)$_2$(R2)$_2$]*, 7**

This compound was synthesized by following a procedure similar to that described above for **1** using **L1** (130 mg, 0.70 mmol), CuI (134 mg), and 4-(diphenylphosphino)benzoic acid (215 mg), yielding **7** as a brown solid (0.31 g, 64%). IR (ATR, diamond): ν/cm^{-1} 2204 (–C≡C–), 1701 (-**C=O**(OH)).^{1}H NMR (700 MHz, $CDCl_3$): δ/ppm 9.60 (s, 2H of COO*H*), 7.73 – 7.67 (m, 4H, $H_{\alpha\text{-pyr}}$), 7.59 – 7.48 (m, 32H, P*Ph*$_3$, $H_{\beta\text{-pyr}}$), 7.23 (m, J = 6.0 Hz, 2H), 7.15 (d, *J* = 3.8 Hz, 4H).^{13}C NMR (700 MHz, $CDCl_3$): δ/ppm 169.3 (C of COOH), 149.4, 136.1, 135.9, 134.0, 132.0, 131.5, 130.7, 130.3, 128.8, 127.9, 127.7, 127.2, 126.2, 122.4 (Aromatic C), 94.01, 88.97(–C≡C–).^{31}PNMR (121.53 MHz, $CDCl_3$): δ = 29.20 (s, P*Ph*$_3$) ppm. ESI-MS: m/z 1366.5. Anal. Calc. for $C_{60}H_{44}Cu_2I_2N_2O_4P_2S_2$: C, 52.83; H, 3.25; N, 2.05%; found: C, 52.71; H, 3.23; N, 2.08%.

***[(CuI)$_2$(L2)$_2$(R2)$_2$]*, 8**

This compound was synthesized by following a procedure similar to that described above for **1** using **L2** (100 mg, 0.37 mmol), CuI (71 mg), and 4-(diphenylphosphino)benzoic acid (115 mg), yielding **8** as light yellow solid (0.20 g, 71%). IR (ATR, diamond): ν/cm^{-1} 2196 (–C≡C–), 1723(-**C=O**(OH)).^{1}H NMR (700 MHz, $CDCl_3$): δ/ppm 9.48 (s, 2H of COO*H*), 7.71 (dd, *J* = 5.6, 3.3 Hz, 4H, $H_{\alpha\text{-pyr}}$), 7.55 – 7.34 (m, 32H, P*Ph*$_3$, $H_{\beta\text{-pyr}}$), 7.34 (s, 2H), 7.23 (d, *J* = 3.6 Hz, 4H), 7.29 (s, 2H), 7.10 (d, *J* = 3.8 Hz, 2H), 7.05 (dd, *J* = 5.1, 3.7 Hz, 2H). ^{13}C NMR (700 MHz, $CDCl_3$): δ/ppm 169.8 (C of COOH), 149.81, 138.54, 136.90, 136.22, 135.90, 134.26, 132.91, 131.53, 130.83, 130.44, 128.82, 128.01, 127.91, 126.45, 124.83, 124.11, 123.54, 122.31(Aromatic C), 95.12, 90.03(–C≡C–).^{31}PNMR (121.53 MHz, $CDCl_3$): δ = 29.21 (s, P*Ph*$_3$) ppm. ESI-MS: m/z 1525.30. Anal. Calc. for $C_{68}H_{48}Cu_2I_2N_2O_4P_2S_4$: C, 53.44; H, 3.17; N, 1.83%; found: C, 53.33; H, 3.13; N, 1.88%.

***[(CuI)$_2$(L3)$_2$(R2)$_2$]*, 9**

This compound was synthesized by following a procedure similar to that described above for **1** using **L3** (90 mg, 0.28 mmol), CuI (53 mg), and 4-(diphenylphosphino)benzoic acid (73 mg),

yielding **9** as a light yellow solid (0.16 g, 67%). IR (ATR, diamond): ν/cm^{-1} 2198 (–C≡C–), 1701(-**C=O**(OH)). ^{1}H NMR (700 MHz, $CDCl_3$): δ/ppm 9.23 (s, 2H of COO*H*), 8.60-8.57 (m, 4H,$H_{\alpha\text{-pyr}}$), 7.92-7.40 (m,26H, P*Ph*$_3$), 7.67 (dd, *J* = 4.9 Hz, 1.2 Hz, 4H, $H_{\beta\text{-pyr}}$), 7.41-7.35 (m, 4H), 7.22 – 7.26 (m, 4H), 7.15 (d, *J* = 4.2 Hz, 4H), 7.10 (d, *J* = 3.8 Hz, 2H), 6.99 (d, *J* = 2.9 Hz, 2H).^{13}C NMR (700 MHz, $CDCl_3$): δ/ppm 169.72 (C of COOH), 149.80, 138.50, 137.91, 136.61, 136.44, 135.87, 134.74, 132.90, 131.82, 130.84, 130.48, 128.62, 128.01, 127.91, 126.43, 125.82, 124.51, 124.10, 123.54, 122.10 (Aromatic C), 97.33, 94.68(–C≡C–).^{31}PNMR (121.53 MHz, $CDCl_3$): δ = 29.15 (s, P*Ph*$_3$) ppm. ESI-MS: m/z 1690.5. Anal. Calc. for $C_{76}H_{52}Cu_2I_2N_2O_4P_2S_6$: C, 53.93; H, 3.10; N, 1.66%; found: C, 53.79; H, 3.13; N, 1.68%.

***[(CuI)$_2$(L3)$_2$(R3)$_2$]*, 10**

This compound was synthesized by following a procedure similar to that described above for **1** using **L3** (100 mg, 0.29 mmol), CuI (55 mg), and 2-(diphenylphosphino)benzenesulfonic acid (99 mg), yielding **12** as a light yellow solid (0.15 g, 59%). IR (ATR, diamond): ν/cm^{-1} 2200 (–C≡C–), 1481, 1168 (-**S=O**(O)(OH)). ^{1}H NMR (700 MHz, $CDCl_3$): δ/ppm9.59 (s, 2H of SO_3H), 8.45 (dd,*J* = 5.1 Hz, 1.3 Hz, 2H, $H_{\alpha\text{-pyr}}$), 8.21 (d, *J* = 6.1 Hz, 2H, $H_{\alpha\text{-pyr}}$), 7.73-7.50 (m, 32H,P*Ph*$_3$, $H_{\beta\text{-pyr}}$), 7.40 – 7.36 (m, 4H), 7.17 (d, *J* = 5.2 Hz, 4H), 7.12 –7.09 (m, 4H), 6.99 (d, *J* = 4.1 Hz, 2H).^{13}C NMR (700 MHz, $CDCl_3$): δ/ppm 145.6 (C of (-S=O(O)(OH)), 149.8, 138.5, 137.9, 136.6, 136.4, 135.8, 134.7, 132.9, 131.8, 130.8, 130.4, 128.6, 128.0, 127.9, 126.4, 125.8, 124.5, 124.1, 123.5, 122.1(Cs of Aromatics), 96.39, 94.08 (–C≡C–).^{31}PNMR (121.53 MHz, $CDCl_3$): δ = 29.14 (s, P*Ph*$_3$) ppm. ESI-MS: m/z 1766.7. Anal. Calc. for $C_{74}H_{52}Cu_2I_2N_2O_6P_2S_8$: C, 50.37; H, 2.97; N, 1.59%;found: C, 50.39; H, 3.03; N, 1.61%.

X-ray crystallography

Single-crystal X-ray structure determinations were performed on **1**, **2**, **4**, and **5**, at 150 K, and **6** at 120 K on a Rigaku Oxford Diffraction Xcalibur CCD diffractometer, for **1**, **4** and **5**, and on a Stoe IPS II diffractometer for **6**, using monochromatic Mo-Kα radiation (λ = 0.71073 Å), and on an Rigaku Oxford Diffraction SuperNova CCD diffractometer, with Cu-Kα radiation (λ = 1.54178 Å) for **2**. The sample temperature was controlled using an Oxford Diffraction Cryojet apparatus. A multi-scan absorption correction was applied in all cases.

The data reduction, including an empirical absorption correction using spherical harmonics, implemented in *SCALE3 ABSPACK* scaling algorithm,[15] was performed using the *CrysAlisPro* software package.[16] The crystal structures were solved by direct methods using the online version

of *AutoChem 2.0* in conjunction with *OLEX2* suite of programs implemented in the *CrysAlis* software,[17] and then refined by full-matrix least-squares (*SHELXL2014*) on F^2.[18] The non-hydrogen atoms were refined anisotropically. All of the hydrogen atoms were positioned geometrically in idealized positions and refined with the riding model approximation, with U_{iso}(H) = 1.2 or 1.5 U_{eq}(C). For the structure of 4 only poor quality crystals could be obtained and a low resolution structure is reported. In this structure the geometry is clearly defined although there are larger errors on the bond parameters than in the other structures reported. For the molecular graphics the program MERCURY, from the CSD package was used.[19]

Voltammetry

Electrochemical experiments were carried out with an Autolab potentiostat type III using software GPES. Cyclic voltammetry (CV) and differential pulse voltammetry (DPV) experiments were conducted in a three-electrode cell using glassy carbon (GC, 3 mm diameter, BASi) and Pt-wire electrodes as working and counter electrode, respectively. An Ag wire electrode was used as a quasi-reference electrode. The samples were dissolved in dry acetonitrile containing 0.1 M tetrabutylammonium hexafluorophosphate (Bu_4NPF_6) as supporting electrolyte. The electrolytic solution was purged with Ar gas for 15 min before performing CV or DPV analysis in order to remove any dissolved oxygen. All experiments were carried out under an inert Ar atmosphere at 298 K. Any presence of air bubbles inside the glass assembly was removed by gently tapping the electrode body.

Computational modeling

All the electronic structure calculations were carried out with Gaussian09. The structural optimization of Cu-complexes has been carried out at the B3LYP level of theory with the 6-31G(d) basis set. The calculated values of the HOMO-LUMO energy gap are presented in **Table 1**. UV-vis spectra of the Cu-complexes were calculated with TD-DFT calculations using the B3LYP level of theory with the 6-31G(d) basis set in the gas phase, CH_2Cl_2, toluene, and water solvent systems with the polarizable continuum model (PCM) as implemented in Gaussian09. By default, the PCM model builds up the cavity using the united atom (UA0) model, i.e., putting a sphere around each solute heavy atom; hydrogen atoms are enclosed in the sphere of the atom to which they are bonded.

Solar Cell

Fabrication of the DSSCs

The working electrode was composed of a 16 μm thick TiO_2 film, including a 12 μm transparent layer with 18 NRT and 4μm scattering layer with 18NR-AO. The dye solutions were 0.3 mM in dichloromethane and the photo-anodes underwent dipping for 12 h to complete the loading with sensitizers. The DSSCs were assembled a sandwich structure with dyed TiO_2 films and Pt-counter electrode, finally sealed with thermal adhesive films of 30μm Surlyn 1702(DuPont) by hot pressing technique. The volatile liquid electrolyte was composed of 0.6 M BMII (1-butyl-3-methylimidazoliumiodide), 0.1 M DMPII (1, 2-dimethyl-3-propylimidazolium iodide), 0.05 M I_2, 0.1 M LiI, 0.1 M GuSCN (guanidinium thiocyanate) and 0.5 M 4-tert-butylpyridine (TBP) in a mixture of acetonitrile(AN) and valeronitrile(volume ratio, 85:15). The platinum counter electrodes were obtained by spin-coating H_2PtCl_6 isopropanol solution (0.02 M) on the FTO glass with sintering at 400°C for 15 min. The liquid electrolyte was injected through the holes on the counter electrode, which were sealed by an aluminum foil tape at last.

Solar simulator

Photovoltaic measurements were illuminated with a solar simulator, 300W xenon lamp (Model No.91160, Oriel).The power of the simulated light was calibrated to 100 mW cm^{-2} by using a Newport Oriel PV reference cell system (Model 91150 V). J-V curves were obtained by applying an external bias to the cells and measuring the generated photocurrent with a Keithley model 2400 digital source meter. The voltage step and delay time of the photocurrent were 10 mV and 40 ms, respectively. The measurement of the incident photon-to-current conversion efficiency (IPCE) of the DSSCs was determined by a QE/IPCE Measurement with a Newport-74125 system (Newport Instruments).

ASSOCIATED CONTENT

Supporting Information

The Supporting Information is available free of charge on the ACS Publications website as DOI: 10.1021/acs.inorgchem.xxxxxxx.

Table of crystal data information, data collection and refinement parameters for compounds **1**, **2**, **4**, **5** and **6**.

X-ray crystallographic data in CIF format for CCDC (1834959 (CIF)

X-ray crystallographic data in CIF format for CCDC (1834960 (CIF)

X-ray crystallographic data in CIF format for CCDC (1834961 (CIF)

X-ray crystallographic data in CIF format for CCDC (1834962 (CIF)

X-ray crystallographic data in CIF format for CCDC (1834963 (CIF)

Accession Codes

Crystallographic data from the structural analyses have been deposited with the Cambridge Crystallographic Data Centre as CCDC1834959-1834963 and are available free of charge from https://summary.ccdc.cam.ac.uk/structure-summary-form.

AUTHOR INFORMATION

Corresponding Authors

*E-mail: msk@squ.edu.om

*E-mail: shahidul321@gmail.com

*E-mail: wai-yeung.wong@polyu.edu.hk, ORCHID ID: 0000-0002-9949-7525

*E-mail: f.marken@bath.ac.uk

*E-mail: p.r.raithby@bath.ac.uk, ORCHID ID: 0000-0002-2944-0662

Notes

The authors declare no competing financial interests

ACKNOWLEDGEMENTS

MSK thanks The Research Council (TRC), Oman (Grant No. ORG/EI/SQU/13/015) and His Majesty's Trust Fund for Strategic Research (Grant No.SR/SQU/SCI/CHEM/16/02) for funding. MJ acknowledges the TRC, Oman for a PhD scholarship and RAA acknowledges Sultan Qaboos University, Oman for PhD scholarship. W.-Y.W. acknowledges the financial support from the Areas of Excellence Scheme of the University Grants Committee of HKSAR (AoE/P-03/08), Hong Kong Research Grants Council (PolyU 153051/17P), the Hong Kong Polytechnic University (1-ZE1C) and Ms. Clarea Au for the Endowed Professorship (847S). PRR and FM are grateful to the Engineering and Physical Sciences Research Council, UK, for funding through an EPSRC Programme Grant (Grant EP/K004956/1).

References

1. Yam, V. W.-W.; Au, V. K.-M.; Leung, S. Y.-L. Light-Emitting Self-Assembled Materials Based on d^8 and d^{10} Transition Metal Complexes. *Chem. Rev.* **2015**, *115* (15), 7589-7728.
2. Haque, A.; Al-Belushi, R. A.; Al-Busaidi, I. J.; Khan, M. S.; Raithby, P. R. Rise of Conjugated Poly-ynes and Poly(Metalla-ynes): From Design Through Synthesis to Structure-Property Relationships and Applications. *Chem. Rev. (Accepted, in-press,* **2018***) (DOI: http://dx.doi.org/10.1021/acs.chemrev.8b00022)*.

3. Liu, Y.; Yiu, S.-C.; Ho, C.-L.; Wong, W.-Y. Recent advances in copper complexes for electrical/light energy conversion. *Coord. Chem. Rev.* **2018**. (*DOI: https://doi.org/10.1016/j.ccr.2018.05.010*).
4. Rath, N. P.; Maxwell, J. L.; Holt, E. M. Fluorescent copper(I) complexes: an X-ray diffraction study of complexes of copper(I) iodide and pyridine derivatives of rhombic,$[Cu_2I_2(3Me\text{-}py)_4]$, and polymeric structure, $[\{CuI(2me\text{-}py)\}_\infty]$ and $[\{CuI(2,4Me_2\text{-}py)\}_\infty]$. *J. Chem. Soc., Dalton Trans.* **1986**, (11), 2449-2453.
5. Safko, J. P.; Kuperstock, J. E.; McCullough, S. M.; Noviello, A. M.; Li, X.; Killarney, J. P.; Murphy, C.; Patterson, H. H.; Bayse, C. A.; Pike, R. D. Network formation and photoluminescence in copper(i) halide complexes with substituted piperazine ligands. *Dalton Trans.* **2012**, *41* (38), 11663-11674.
6. Waterland, M. R.; Flood, A.; Gordon, K. C. Metal-to-ligand charge-transfer excited-states in binuclear copper(I) complexes. Tuning MLCT excited-states through structural modification of bridging ligands. A resonance Raman study. *J. Chem. Soc. Dalton Trans.* **2000**, (2), 121-127.
7. Ford, P. C.; Cariati, E.; Bourassa, J. Photoluminescence properties of multinuclear copper(I) compounds. *Chem. Rev.* **1999**, *99* (12), 3625-3648.
8. Chaurin, V.; Constable, E. C.; Housecroft, C. E. What is the coordination number of copper(ii) in metallosupramolecular chemistry? *New J. Chem.* **2006**, *30* (12), 1740-1744.
9. Ilmi, R.; Al-Busaidi, I. J.; Haque, A.; Khan, M. S. Recent Progress in Coordination Chemistry, Photo-physical Properties and Applications of Pyridine-Based Cu(I) Complexes. J. *Coord. Chem. (in-press,* **2018***)*. (DOI: *https://doi.org/10.1080/00958972.2018.1509070*).
10. Haque, A.; Ilmi, R.; Al-Busaidi, I. J.; Khan, M. S. Coordination chemistry and application of mono-and oligopyridine-based macrocycles. *Coord. Chem. Rev.* **2017**, *350* (1), 320-339.
11. Hostettler, N.; Wright, I. A.; Bozic-Weber, B.; Constable, E. C.; Housecroft, C. E. Dye-sensitized solar cells with hole-stabilizing surfaces: "inorganic" versus "organic" strategies. *RSC Adv.* **2015**, *5* (47), 37906-37915.
12. Constable, E. C.; Redondo, A. H.; Housecroft, C. E.; Neuburger, M.; Schaffner, S. Copper(i) complexes of 6,6′-disubstituted 2,2′-bipyridine dicarboxylic acids: new complexes for incorporation into copper-based dye sensitized solar cells (DSCs). *Dalton Trans.* **2009**, (33), 6634-6644.
13. Bessho, T.; Constable, E. C.; Graetzel, M.; Redondo, A. H.; Housecroft, C. E.; Kylberg, W.; Nazeeruddin, M. K.; Neuburger, M.; Schaffner, S. An element of surprise-efficient copper-functionalized dye-sensitized solar cells. *Chem. Commun.* **2008**, (32), 3717-3719.
14. Housecroft, C. E.; Constable, E. C. The emergence of copper(I)-based dye sensitized solar cells. *Chem. Soc. Rev.* **2015**, *44* (23), 8386-8398.
15. Bozic-Weber, B.; Constable, E. C.; Housecroft, C. E. Light harvesting with Earth abundant d-block metals: Development of sensitizers in dye-sensitized solar cells (DSCs). *Coord. Chem. Rev.* **2013**, *257* (21), 3089-3106.
16. Magni, M.; Biagini, P.; Colombo, A.; Dragonetti, C.; Roberto, D.; Valore, A. Versatile copper complexes as a convenient springboard for both dyes and redox mediators in dye sensitized solar cells. *Coord. Chem. Rev.* **2016**, *322*, 69-93.

17. Cao, Y.; Saygili, Y.; Ummadisingu, A.; Teuscher, J.; Luo, J.; Pellet, N.; Giordano, F.; Zakeeruddin, S. M.; Moser, J.-E.; Freitag, M. 11% efficiency solid-state dye-sensitized solar cells with copper(II/I) hole transport materials. *Nat. Commun.* **2017**, *8*, 15390.
18. Li, J.; Yang, X.; Yu, Z.; Gurzadyan, G. G.; Cheng, M.; Zhang, F.; Cong, J.; Wang, W.; Wang, H.; Li, X. Efficient dye-sensitized solar cells with [copper(6,6′-dimethyl-2,2′-bipyridine)$_2$]$^{2+/1+}$ redox shuttle. *RSC Adv.* **2017**, *7* (8), 4611-4615.
19. Shah, H. H.; Al-Balushi, R. A.; Al-Suti, M. K.; Khan, M. S.; Marken, F.; Sudlow, A. L.; Kociok-Köhn, G.; Woodall, C. H.; Raithby, P. R.; Molloy, K. C. New di-ferrocenyl-ethynylpyridinyl triphenylphosphine copper halide complexes and related di-ferricenyl electro-crystallized materials. *Dalton Trans.* **2014**, *43* (25), 9497-9507.
20. Shah, H. H.; Al-Balushi, R. A.; Al-Suti, M. K.; Khan, M. S.; Woodall, C. H.; Sudlow, A. L.; Raithby, P. R.; Kociok-Köhn, G.; Molloy, K. C.; Marken, F. New Multi-Ferrocenyl- and Multi-Ferricenyl-Materials via Coordination-Driven Self-Assembly and via Charge-Driven Electro-Crystallization. *Inorg. Chem.* **2013**, *52* (20), 12012-12022.
21. Fery-Forgues, S.; Delavaux-Nicot, B. Ferrocene and ferrocenyl derivatives in luminescent systems. *J. Photochem. Photobiol. Chem.* **2000**, *132* (3), 137-159.
22. Albagli, D.; Bazan, G.; Schrock, R.; Wrighton, M. New functional polymers prepared by ring-opening metathesis polymerization: study of the quenching of luminescence of pyrene end groups by ferrocene or phenothiazine centers in the polymers. *J. Phys. Chem.* **1993**, *97* (39), 10211-10216.
23. Giasson, R.; Lee, E. J.; Zhao, X.; Wrighton, M. S. Inter-and intramolecular quenching of the singlet excited state of porphyrins by ferrocene. *J. Phys. Chem.* **1993**, *97* (11), 2596-2601.
24. Al-Balushi, R. A.; Haque, A.; Jayapal, M.; Al-Suti, M. K.; Husband, J.; Khan, M. S.; Koentjoro, O. F.; Molloy, K. C.; Skelton, J. M.; Raithby, P. R. Experimental and theoretical investigation for the level of conjugation in carbazole-based precursors and their mono-, di-, and polynuclear Pt(II) complexes. *Inorg. Chem.* **2016**, *55* (13), 6465-6480.
25. Hsu, S.-H.; Reinhoudt, D. N.; Huskens, J.; Velders, A. H. Lateral interactions at functional monolayers. *J. Mater. Chem.* **2011,** *21* (8), 2428-2444.
26. Eyley, S.; Shariki, S.; Dale, S. E.; Bending, S.; Marken, F.; Thielemans, W. Ferrocene-decorated nanocrystalline cellulose with charge carrier mobility. *Langmuir* **2012**, *28* (16), 6514-6519.
27. Sudha Devi, L.; Al-Suti, M. K.; Zhang, N.; Teat, S. J.; Male, L.; Sparkes, H. A.; Raithby, P. R.; Khan, M. S.; Köhler, A. Synthesis and comparison of the optical properties of platinum (II) poly-ynes with fused and non-fused oligothiophenes. *Macromolecules* **2009**, *42* (4), 1131-1141.
28. Ruaa M., A.; Ghadah, A.; Daniela Vargas, T.; Vladimir N., N.; Manal A., R.-O. New Coordination Polymers of Copper(I) and Silver(I) with Pyrazine and Piperazine: A Step Toward "Green" Chemistry and Optoelectronic Applications. **2018**. (DOI: *10.1021/acs.inorgchem.8b01131*)
29. GaussView, V.; Roy D.; Todd A. K.; John M. M. Semichem Inc., Shawnee Mission, KS, **2016**.
30. Wills, K. A.; Mandujano-Ramírez, H. J.; Merino, G.; Oskam, G.; Cowper, P.; Jones, M. D.; Cameron, P. J.; Lewis, S. E. What difference does a thiophene make? Evaluation of a 4,4′-bis(thiophene) functionalised 2,2′-bipyridyl copper(I) complex in a dye-sensitized solar cell. *Dyes Pigm.* **2016**, *134*, 419-426.

31. Lu, X.; Wei, S.; Wu, C.-M. L.; Li, S.; Guo, W. Can polypyridyl Cu(I)-based complexes provide promising sensitizers for dye-sensitized solar cells? A theoretical insight into Cu(I) versus Ru(II) sensitizers. *J. Phys. Chem. C* **2011,** *115* (9), 3753-3761.
32. Yanagi, H.; Chen, S.; Lee, P. A.; Nebesny, K. W.; Armstrong, N. R.; Fujishima, A. Dye-sensitizing effect of TiOPc thin film on n-TiO_2 (001) surface. *J. Phys. Chem.* **1996**, *100* (13), 5447-5451.
33. Liu, R.; Azenkeng, A.; Zhou, D.; Li, Y.; Glusac, K. D.; Sun, W. Tuning photophysical properties and improving nonlinear absorption of Pt(II) diimine complexes with extended π-conjugation in the acetylide ligands. *J. Phys. Chem. A* **2013**, *117* (9), 1907-1917.

For Table of Contents Only

Table of Content Graphic

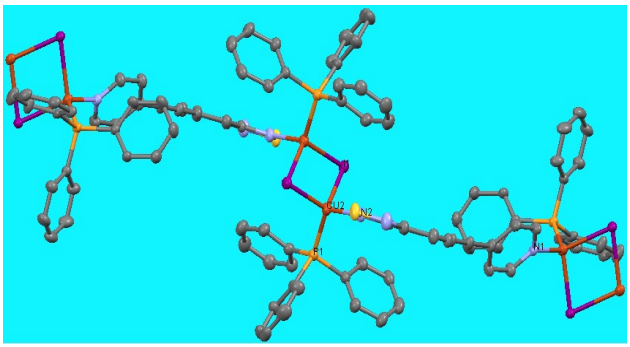

Table of Content Synopsis

The synthesis, structural and photovoltaic characterization of a series of acetylide-functionalized pyridinyl ligands incorporating conjugated heteroaryl spacers and their Cu(I) complexes is reported. The impact of structural variation on solid-state packing and DSSC properties is studied in detail.